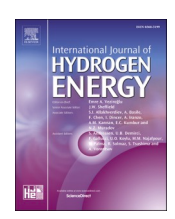
ELSEVIER

Contents lists available at ScienceDirect

International Journal of Hydrogen Energy

journal homepage: www.elsevier.com/locate/he





Multi-option analytical modeling of levelized costs across various hydrogen supply chain nodes

Pietro Dogliani ^a, Afonso Nolan Ruas Rego Canha ^a, Ahmed M. Elberry ^{b,c}, Jagruti Thakur ^{a,*}

- ^a Department of Energy Technology, KTH Royal Institute of Technology, Stockholm, Sweden
- ^b Faculty of Science (HIMS), University of Amsterdam, Amsterdam, the Netherlands
- ^c TNO Energy and Materials Transition, Amsterdam, the Netherlands

ARTICLE INFO

Handling Editor: Prof. J. W. Sheffield

ABSTRACT

Hydrogen is envisioned to become a fundamental energy vector for the decarbonization of energy systems. Two key factors that will define the success of hydrogen are its sustainability and competitiveness with alternative solutions. One of the many challenges for the proliferation of hydrogen is the creation of a sustainable supply chain. In this study, a methodology aimed at assessing the economic feasibility of holistic hydrogen supply chains is developed. Based on the designed methodology, a tool which calculates the levelized cost of hydrogen for the different stages of its supply chain: production, transmission & distribution, storage and conversion is proposed. Each stage is evaluated individually, combining relevant technical and economic notions such as learning curves and scaling factors. Subsequently, the findings from each stage are combined to assess the entire supply chain as a whole. The tool is then applied to evaluate case studies of various supply chains, including large-scale remote and small-scale distributed green hydrogen supply chains, as well as conventional steam methane reforming coupled with carbon capture and storage technologies. The results show that both green hydrogen supply chains and conventional methods can achieve a competitive LCOH of around $\varepsilon 4/kg$ in 2030. However, the key contribution of this study is the development of the tool, which provides a foundation for a comprehensive evaluation of hydrogen supply chains that can be continuously improved through the inputs of additional users and further research on one or more of the interconnected stages.

1. Introduction

With the rising concern to limit global warming to 1.5 °C, countries around the world are facing unprecedented challenges. To fulfil their commitments under the Paris agreement, a deep decarbonization and rapid energy transition is necessary, involving all sectors and systems [1]. As such, alternative solutions to fossil fuels are needed, and hydrogen has become a promising candidate as an energy carrier that can be produced from zero- and low-carbon sources and adapted to meet the needs of different applications. Specifically, its potential to decarbonize hard-to-abate sectors gives it a central role in the efforts toward decarbonizing energy systems. However, despite technological advancements and cost reductions, the path to hydrogen's competitiveness as an energy carrier and its large-scale deployment remains unclear [2].

Currently, hydrogen is mainly used as a reagent in various industrial processes, with the two largest uses being ammonia production and fossil fuel refining [3]. The global demand for pure hydrogen is around

90 Mt per year, with 96% of it produced from fossil fuels [4]. This translates into 900 Mt of carbon dioxide (CO_2) emitted per year [3]. The future increase in hydrogen demand requires a shift to cleaner production processes, such as water electrolysis powered with renewable electricity, pyrolysis, or conventional methods (e.g. steam methane reforming) coupled with carbon capture and storage (CCS) technologies [3].

A strong hydrogen market is closely linked to the availability of reliable infrastructure that would ensure the security of supply and flexibility to the end users. Both efficient delivery and storage options are therefore crucial. Hydrogen transmission and distribution (T&D) involves similar methods to those of natural gas, namely pipelines and its shipping in liquid form. Trucks are also a possibility for shorter distances. Complementarily to transportation, the link between supply and demand is further secured by storage options. Depending on the size and duration, both geological sites and pressure vessels are under investigation.

E-mail address: jrthakur@kth.se (J. Thakur).

https://doi.org/10.1016/j.ijhydene.2024.05.142

^{*} Corresponding author.

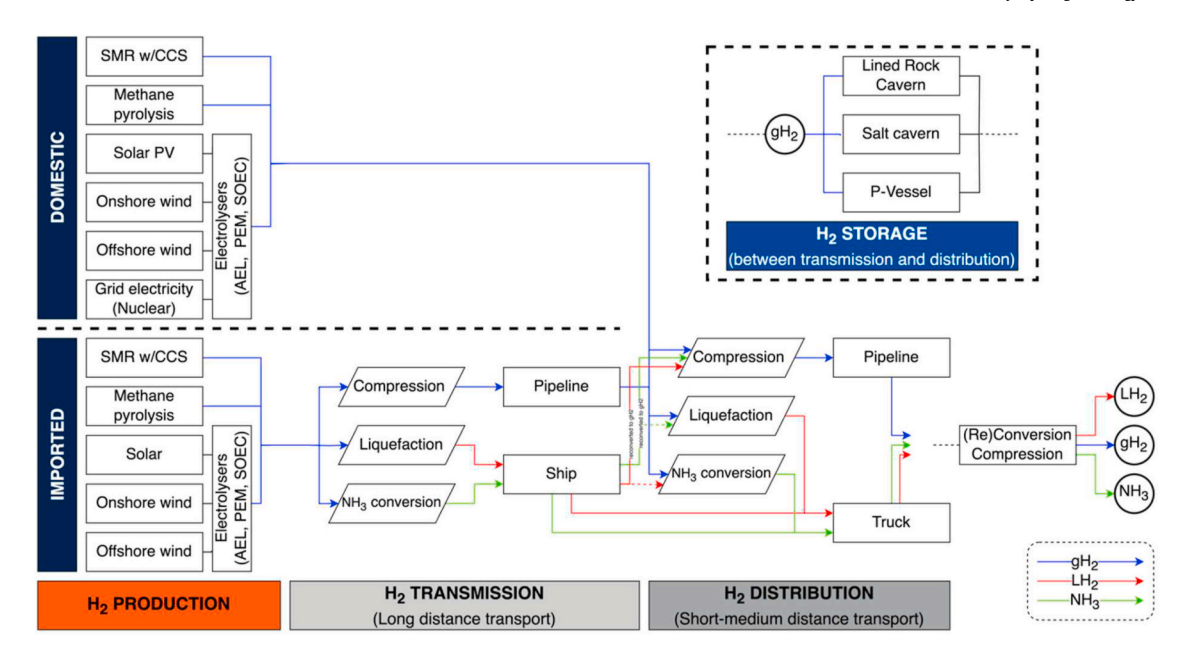


Fig. 1. Tool scope and possible hydrogen supply pathways.

This paper aims to study the whole hydrogen supply chain to assess its costs with the key indicator being the levelized cost of hydrogen (LCOH). For each stage, several options are considered, and the impact of some key parameters is analyzed. The paper is organized as follows: a literature review is provided in Subsection 1.1; Section 2 provides a brief description of each stage, the methodology adopted to study it, and the supply pathways considered; Section 3 presents the results, and finally, Section 4 concludes the paper with final remarks.

1.1. Literature review

Several studies have explored the hydrogen supply chain using two main approaches, optimization and linear modeling. Stockl et al. [5] optimized and compared large- and small-scale hydrogen production from grid electricity. The study showed that small-scale on-site electrolysis is the most beneficial when there are low shares of renewable energy in the electricity mix and low hydrogen demand. For higher renewable shares or higher hydrogen demand, large-scale production becomes more favorable. In particular, liquid hydrogen (LH₂) results to be the best solution with these settings due to its high efficiency, flexibility, and investment costs. Almansoori and Shah [6] also formulated a similar optimization problem, but only considered conventional methods for hydrogen production. They found that the optimal supply chain comprises medium-to-large centralized steam methane reforming (SMR) plants for hydrogen production, distributed via LH₂ tanker trucks and stored in centralized storage sites.

On the other hand, Brändle et al. [7] followed a linear approach to estimate hydrogen supply costs until 2050. They found that in the medium term, SMR will be the cheapest option, while hydrogen from electrolysis could become competitive in the long term, with production cost below 1 \$/kg in some regions. To transport such hydrogen to Europe, retrofitting natural gas pipelines would provide the opportunity for a low-cost transportation method, especially compared to shipping options. The authors suggest that these would lead to the development of a regional market, rather than a global exchange.

A plethora of studies focused on a single stage of the hydrogen supply chain, such as production or transmission. Janssen et al. [8] showed a potential cost decline to produce renewable hydrogen in various European countries, from a current range of 2.1–15 ϵ /kg to a LCOH well below 2 ϵ /kg in 2050. The Hydrogen Council [2] predicted a similar trend for Europe, from 5.5 ϵ /kg today to 2.3 ϵ /kg in 2030. Meanwhile,

the International Energy Agency (IEA) [3] compared different transmission carriers and modes for hydrogen, concluding that the most economical option depends greatly on the distance of transmission, the form of hydrogen being transported, and the additional costs of conversion and reconversion.

Calculating the LCOH is a fundamental and essential step of optimizing the hydrogen supply chain. It involves assessing capital investment, operating costs, hydrogen production analysis, transportation and storage expenses, feedstock costs, and potential revenue streams. By synthesizing data and assumptions from these stages, a comprehensive LCOH analysis is derived. This in-depth evaluation facilitates informed comparisons between various hydrogen production methods and supply chain configurations, thereby aiding in making optimal decisions.

Despite the considerable body of literature concerning specific stages and technologies within the hydrogen supply chain, a holistic and allencompassing calculation, spanning from production to final distribution, remains largely unexplored. For instance, existing studies have analyzed the hydrogen supply chain from production to storage, but often with limited options for production technologies [9-13], transportation methods [14-16], and storage solutions [17-19]. Furthermore, a majority of these studies have neglected to account for hydrogen's final distribution or its levelized cost when imported from other countries. As such, this research seeks to address this knowledge gap by presenting a user-friendly, replicable, and scalable tool designed to bridge the existing literature divide. The proposed tool not only calculates the LCOH while providing a range of technological options for each stage, including final distribution, but also enables the evaluation of LCOH when hydrogen is imported from North Africa, the Middle East, Latin America, and Southern Europe. The tool takes into consideration various factors, such as production means/technologies, feedstock sources in the exporting country, transportation distances, and methods, as well as other comprehensive details essential for a thorough analysis. By offering such an integrated and comprehensive approach, this research contributes novel insights to the field of hydrogen supply chain optimization.

2. Methodology

This section briefly introduces the different stages of the hydrogen supply chain and presents a methodology to evaluate its overall cost. The supply chain is divided in four stages: production, transmission and distribution (T&D), storage, and conversion. For each stage, different technologies are identified (see Fig. 1). Subsection 2.1 expands on the concept of LCOH, which the key indicator we used in assessing the cost of hydrogen. Subsections 2.2 to 2.5 then delve into each of the four stages and their respective technologies, and detail the distinct approaches used to assess their associated costs. The different stages, and their costs, are then aggregated with different combinations, referred to as hydrogen pathways, which serve as case studies to illustrate the potential of the proposed tool.

As highlighted before, the focal point of this research is the development of the tool that incorporates calculations for each stage and integrates their results to provide the overall cost for a chosen pathway. The tool is described in detail in Subsection 2.6 and the examined pathways in Subsection 2.7.

2.1. The levelized cost of hydrogen

In the context of cost analysis, *Levelized* refers to the practice of accounting for the time value of money. This concept originates from the levelized cost of electricity (LCOE), which calculates the average cost per unit of electricity produced by an energy system over its lifetime. The LCOE approach provides a consistent and standardized metric for comparing the costs of different energy sources and enables decision-makers to identify the most economically viable options [20]. The LCOE formula has been adapted for use in the analysis of the cost of hydrogen production and delivery [21]:

$$LCOH = \frac{NPV_{cost}}{NPV_{H_2}} = \frac{\sum_{n=0}^{N} \frac{C_n}{(1+d)^n}}{\sum_{n=0}^{N} \frac{Q_{H_{2,n}}}{(1+d)^n}}$$
(1)

where NPV is the net present value; C_n is the sum of the system costs in the year n; $Q_{H2,n}$ is the annual amount of hydrogen handled; N is the system economic lifetime; and d is the discount rate. Assuming that the system starts to operate one year from its construction (i.e., the sheer, initial investment occurs in year 0), and that costs and quantities of hydrogen handled are constant throughout the years of operation, Equation (1) can be rewritten as:

$$LCOH = \frac{(a_{\%} + OPEX_{\%}) \cdot CAPEX}{Q_{H_{2}}}$$
 (2)

where $OPEX_{\%}$ are the operating expenditures, expressed as a percentage of the CAPEX; and $a_{\%}$ is the amortization factor, function of the discount rate d and the economic lifetime N:

$$a_{\%} = \frac{1}{\sum_{i} \frac{1}{(1+d)^{n}}} = \frac{d}{1 - (d+1)^{-N}}$$
(3)

The use of Equation (2) is restricted to those stages of the hydrogen supply chain where its underlying assumptions hold true, namely, where the operational expenses and hydrogen production remain constant throughout the years. In instances where these assumptions are not met, Equation (1) in combination with cash and hydrogen flow analyses conducted on an annual basis are utilized.

The LCOH is individually calculated for each stage of the hydrogen supply chain, namely.

- LCOH_n: levelized cost of hydrogen production
- LCOH_s: levelized cost of hydrogen storage
- $LCOH_{t\&d}$: levelized cost of hydrogen transportation, sum of the transmission ($LCOH_t$) and distribution ($LCOH_d$) components
- LCOH_{conv}: levelized cost of hydrogen conversion

The LCOH for the whole hydrogen supply chain is then calculated as the sum of these components:

$$LCOH = LCOH_n + LCOH_s + LCOH_{t\&d} + LCOH_{conv}$$
(4)

The capital expenses associated with each technology are a substantial component of the LCOH equation. To investigate the CAPEX of a generic system, it is important to introduce the concept of economy of scale, that has a dual effect on the system costs. First, it influences the manufacturing process as an aspect of technological learning. Its potential to reduce costs is expounded using learning curves, which posit that the cost of a technology reduces by a constant factor, known as the learning rate (LR), with every doubling of the installed capacity [22,23]. The general expression of learning curves for the cost of technology at a specific time t is:

$$c(t) = c_0 \cdot \left(\frac{X(t)}{X_0}\right)^{-b} \tag{5}$$

where c_0 is the cost of the technology at the reference time t_0 ; X(t) is the installed capacity at time t; X_0 is the installed capacity at the reference time t_0 ; b is the slope of the function on a log-log plot and it is related to the LR by:

$$LR = 1 - 2^{-b} (6)$$

Second, the economy of scale can reduce specific unitary investment costs through the upscaling of capacity. This effect is represented by scaling factors [24], which relate the costs of a system with a capacity (size) *S* to the reference one:

$$C = C_{ref} \cdot \left(\frac{S}{S_{ref}}\right)^{sf} \tag{7}$$

2.2. Production

The present study considers three hydrogen production methods: electrolysis, steam methane reforming (SMR), and pyrolysis. Due to the annual fluctuations in some pertinent expenses, such as electricity and gas prices, it is deemed preferable to employ Equation (1) and normalize it per unit of capacity:

$$LCOH_{p} = \frac{\sum_{t=0}^{N} \frac{c_{t}}{(1+d)^{t}}}{\sum_{t=0}^{N} \frac{q_{H2.t}}{(1+d)^{t}}}$$
(8)

The unit of capacity for electrolysis is denoted by power consumption (kW_{el}), whereas for SMR and pyrolysis, it pertains to production capacity ($kW_{H2,LHV}$). As a result, the calculation of annual hydrogen production for electrolysis is derived based on its power consumption unit, as expressed by Equation (9). Conversely, the annual hydrogen production for both SMR and pyrolysis is computed based on their production capacity, as indicated in Equation (10).

$$q_{H2,t} \left[\frac{kg_{H2}/a}{kW_{el}} \right] = \frac{Q_{H2,t}}{P_{el}} = \frac{\eta_{LHV,t} \cdot CF \cdot 8760h}{LHV_{H2}}$$
(9)

$$q_{H2,t} \left[\frac{kg_{H2}/a}{kW_{H2,LHV}} \right] = \frac{Q_{H2,t}}{P_{H2,t}} = \frac{CF \cdot 8760h}{LHV_{H2}}$$
 (10)

where CF is the electrolyzer capacity factor and $\eta_{LHV.n}$ is its efficiency in the year n. Further details on the efficiency parameter for electrolysis can be found in Appendix I.

The succeeding subsections provide a detailed breakdown of the cost components associated with the three production technologies considered in this study, namely electrolysis, SMR, and pyrolysis. Furthermore, the subsections also expound on the fundamental features of each technology.

Table 1Summary of the main technical parameters, maturity level, advantages and disadvantages of four different electrolyzer technologies [25,26, author's analysis].

	AEL	PEM	SOEC
Temperature	70–90 °C	50–80 °C	700–850 °C
Pressure	1–30 bar	<70 bar	1 bar
Electrolyte	Liquid	Solid, polymeric	Solid, ceramic
Stack efficiency	59-70%	65-82%	Up to 100%
System efficiency [kWh/kg _{H2}]	50–78	50–83	45–55
Maturity level	Commercial	Near-term commercialization	Laboratory scale
Advantages	Low CAPEX, relatively stable, mature technology	Compact design, fast start-up, high-purity H_2	Enhanced kinetics and thermodynamics, lower energy demand
Disadvantages	Corrosive electrolyte, gas permeation, slow dynamics	High-cost polymeric membranes	Mechanically unstable electrodes, safety issues

2.2.1. Electrolysis

Water electrolysis is a process where water splits into hydrogen and oxygen under the influence of direct current. This study considers three electrolysis technologies: alkaline electrolyzer (AEL), proton exchange membrane (PEM), and solid-oxide electrolyzer cell (SOEC). Despite sharing the same operating principle, they differ in technology, materials, applications, and maturity. Table 1 compares the different technologies and their main parameters.

The methodology used to calculate the cost of hydrogen production is composed of the following parameters, which are common to all electrolysis technologies.

- Electrolyzer (whole system) capital expenses
- Fixed operational expenses
- Stack replacement costs
- Electricity costs, either from the grid or from specific RE plant
- Water cost
- Revenues from oxygen sale

Capital expenses: the CAPEX is calculated by combining learning and scaling effects, and dividing the electrolysis system into stacks and auxiliary components. A general formula is used to calculate the CAPEX of a system of size *S* in the year *t*:

$$c_{el,t,S} = c_{el,t_0,S_{ref}} \cdot \left[\%_{st2sys} \cdot (1 + AGR)^{-(t-t_0) \cdot \log_2(1 - LR_{st})} \cdot \left(\frac{S}{S_{ref}} \right)^{(1 - sf_{st,0}) \cdot e^{-S/S_{max}}} + (1 - \%_{st2sys}) \cdot (1 + AGR)^{-(t-t_0) \cdot \log_2(1 - LR_{aux})} \cdot \left(\frac{S}{S_{ref}} \right)^{sf_{aux} - 1} \right]$$

$$(11)$$

where $c_{el,t_0,S_{ref}}$ is the CAPEX of the reference system size S_{ref} in the reference year t_0 ; $\%_{st2sys}$ is the ratio between the stack and the total cost for the reference electrolyzer system; AGR is the annual growth rate for the global electrolyzer production capacity; LR_{st} and LR_{aux} are the learning rates for stack and auxiliary components; $sf_{st,0}$ and sf_{aux} are their scaling factors; $st{S}_{max}$ is the maximum stack size. Appendix I provides a more detailed overview of Equation (11) and its variables.

Fixed operational expenses: the annual fixed OPEX are calculated as a percentage of the initial investment.

Stack replacement costs: the stack typically has a shorter operational lifetime compared to the whole system. For this reason, it is assumed that the stack is replaced after a certain number of load hours. Its cost is equal to the stack component of Equation (11).

Electricity cost: the electrolyzer can either be connected to the grid or to a dedicated Renewable Energy Sources (RES) plant. In the former case, the electricity cost is described by Equation (12), while in the latter case, the electricity cost is added after the cash flow analysis to avoid double accounting for the value of money, as shown in Equation (13).

$$c_{electricity,t} = price_{electricity,t} \cdot CF \cdot 8760 \tag{12}$$

$$LCOH_{p} = \frac{\sum_{n=0}^{N} \frac{c_{n}}{(1+d)^{n}}}{\sum_{n=0}^{N} \frac{q_{H2,n}}{(1+d)^{n}}} + LCOE \cdot \frac{LHV_{H2}}{\eta_{el}}$$
(13)

The electricity cost of the dedicated RES plant, expressed as *LCOE*, is also calculated within the tool, as shown in Appendix I.

Water cost: water cost is calculated based on the stoichiometry of the reaction, where 9 kg of water are required for producing 1 kg of hydrogen [27]. The annual cost of water per kW of hydrogen is thus equal to:

$$c_{H2O}\left[\frac{\epsilon}{kW_{H2,LHV}\cdot a}\right] = c_{H2O}\left[\frac{\epsilon}{L_{H2O}}\right] \cdot \frac{m_{H2O}}{m_{H2}} \cdot q_{H2} \tag{14}$$

Revenues from oxygen sale: In the electrolysis process, 8 kg of oxygen are produced (as a by-product) with every kilogram of hydrogen [28]. As oxygen has various commercial applications, such as in the medical field, additional revenue can be generated from the sale of this by-product. This additional revenue is accounted as a negative cost in the electrolysis cash flow and can be calculated using Equation (15) [28].

$$r_{02} \left[\frac{\epsilon}{kW_{H2,LHV} \cdot a} \right] = - p_{02} \left[\frac{\epsilon}{kg_{02}} \right] \cdot \frac{m_{02}}{m_{H2}} \cdot q_{H2}$$
 (15)

2.2.2. Steam Methane Reforming

The steam reforming process is based on the endothermic reaction of steam and hydrocarbons to produce hydrogen and carbon oxides. In an SMR conventional facility, natural gas is the process feedstock and, in most cases, also the process fuel. Otherwise, also the produced hydrogen can be partly used as fuel [4,29]. To cut the carbon footprint of such

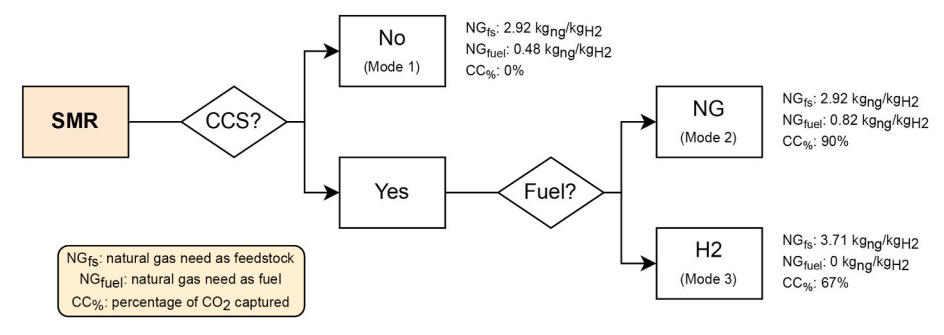


Fig. 2. SMR modes, with related natural gas requirements and carbon capture percentages. Own elaboration, data from Ref. [29].

plants, they can be complemented with carbon capture and storage (CCS). In particular, the most suitable capture technology combined to SMR is gas absorption with amine-based solvents [30].

The SMR process can generate hydrogen with varying levels of carbon emissions depending on its configuration. The present tool models three modes of operation, which are determined by two factors: the presence of a carbon capture plant; and the choice of process fuel, which could be either natural gas or recirculated hydrogen. Fig. 2 depicts the potential combinations and displays the associated ${\rm CO_2}$ emissions and natural gas requirements, as per the scenarios put forth by Collodi et al. [29].

The cost breakdown of the SMR process can be categorized into different components, regardless of the mode of operation.

- Capital expenses
- Fixed operational expenses
- Natural gas cost
- ${\rm CO_2}$ emission price, either from emission trading system or carbon tax
- CO₂ transportation-and-storage costs
- Revenues from combined steam turbine electricity

Capital expenses: the CAPEX of a SMR plant can be divided into the conventional plant components and the carbon capture plant. The notion of economy of scale influences the plant CAPEX due to learning and scaling effects. The learning effects consider only the carbon capture component, since it is assumed that the conventional plant components are well-established technologies and a decrease in their cost is not forecastable ($LR_{conv}=0$). On the other hand, the scaling effect concerns the plant as a whole. The combination of learning and scaling effects is described with the following equation:

needs to be added to the overall costs. The ${\rm CO}_2$ emitted to the atmosphere in a year is equal to:

$$q_{Cem} = q_{Ctot} \cdot (1 - CC_{\%}) \tag{20}$$

where $CC_{\%}$ is the percentage of CO_2 captured, as reported in Fig. 1. The emission tax or price P_C on the total costs is calculated in the following way:

$$c_{C,em} = P_C \cdot q_{C,em} \tag{21}$$

CO₂ transportation-and-storage costs: the captured portion also has a cost associated with its transportation and storage:

$$c_{C,T\&S} \left[\frac{\epsilon}{kW_{H2,LHV}} \right] = c_{C,T\&S} \left[\frac{\epsilon}{t_{CO2}} \right] \cdot q_{C,T\&S} = c_{C,T\&S} \left[\frac{\epsilon}{t_{CO2}} \right] \cdot q_{C,tot} \cdot CC_{\%}$$
 (22)

Revenues from combined steam turbine electricity: the SMR process produces excess steam, that can be converted to electricity in a steam turbine island, and the associated revenue is accounted for as a negative cost:

$$c_{el} = p_{el,feed-in} \cdot el_{cons} \cdot q_{H2} \tag{23}$$

where $p_{el,feed-in}$ is the electricity feed-in tariff and el_{cons} is the electricity consumption. Since the SMR plant is a net electricity producer, this value is negative.

2.2.3. Pyrolysis

Pyrolysis is a thermochemical process characterized by the decomposition of a material at high temperatures in the absence of an oxidizing agent. This process has been widely utilized to produce hydrogen from methane obtained from natural gas, where the only resultant product is elemental hydrogen and solid carbon. The exclusion of oxygen in the

$$c_{SMR} = \left[c_{conv,t_0,S_{ref}} \cdot (1 + AGR)^{-(t-t_0) \cdot \log_2(1 - LR_{conv})} + c_{cc,t_0,S_{ref}} \cdot (1 + AGR)^{-(t-t_0) \cdot \log_2(1 - LR_{cc})}\right] \cdot \left(\frac{S}{S_{ref}}\right)^{sf-1}$$
(16)

where the abbreviations *conv* and *cc* refer respectively to conventional and carbon capture components.

Fixed operational expenses: the annual fixed OPEX are calculated as a percentage of the initial investment.

Natural gas costs: natural gas is the main energy input of the SMR facility, therefore its cost has a significant impact on the plant economics. The annual natural gas consumption is calculated using Equation (17) and the cost associated with it is calculated using Equation (18).

$$q_{ng}\left[\frac{kWh_{ng,HHV}/a}{kW_{H2,LHV}}\right] = \left(q_{ng,fs}\left[\frac{kg_{ng}}{kg_{H2}}\right] + q_{ng,fuel}\left[\frac{kg_{ng}}{kg_{H2}}\right]\right) \cdot CF \cdot 8760h \cdot \frac{HHV_{ng}}{LHV_{H2}}$$

$$(17)$$

$$c_{ng} = P_{ng} \cdot q_{ng} \tag{18}$$

where $q_{ng,fs}$ and $q_{ng,fuel}$ are respectively the gas needed as feedstock and as fuel per unit of output. These values are reported in Fig. 2. P_{ng} is the natural gas price in $\epsilon/kWh_{ng,HHV}$

 CO_2 emissions price: CO_2 is generated as a by-product of the SMR process. A typical plant usually generates annual emissions that is equal to:

$$q_{C,tot} = EF_{ng} \cdot q_{ng} \tag{19}$$

where EF_{ng} is the natural gas emission factor. A part of these emissions gets released into the atmosphere, therefore an emission surcharge

reaction leads to the absence of carbon monoxide (CO) and carbon dioxide (CO2), negating the requirement for further carbon separation units [31].

To narrow the scope, pyrolysis is described in the tool by a single configuration: the molten metal process, despite the existence of alternative methods. Moreover, with the objective of studying a completely CO₂-free process, a hydrogen-fired layout is selected, since other fuel supply options (electricity, natural gas) have direct and indirect emissions. The pyrolysis costs considered in the analysis include.

- Capital expenses
- Fixed operational expenses
- Natural gas cost
- Solid carbon cost (revenues from its sale or disposal costs)

The consumption of electricity and its corresponding costs are deemed negligible as their impact on the overall cash flow for this particular configuration is minimal [31].

Capital expenses: in this case, learning curves are not utilized due to the early development stage of the pyrolysis process. Instead, the Lang factor concept, as described by Parkinson et al. [31], is utilized to determine the plant's CAPEX, based on its technology readiness level (TRL). The total equipment cost is multiplied by the Lang factor, which varies depending on the TRL of the technology. In our tool, a Lang factor

of 10 (first-of-a-kind¹) is used to calculate the CAPEX of the pyrolysis process in 2022. This means that the CAPEX is assumed to be ten times the total equipment cost. The Lang factor is then assumed to decrease linearly to 6 (nth-of-a-kind) by 2030, as the technology becomes more mature, and the costs associated with it decrease. This means that the CAPEX in 2030 is assumed to be six times the total equipment cost.

Fixed operational expenses: the annual fixed OPEX are calculated as a percentage of the initial investment.

Natural gas costs: natural gas is the only input of the process, and its cost is a crucial factor in determining the overall LCOH. The natural gas annual consumption and its corresponding costs are calculated using Equations (24) and (25), respectively.

$$q_{ng} \left[\frac{kWh_{ng,HHV}/a}{kW_{H2,LHV}} \right] = q_{ng} \left[\frac{kg_{ng}}{kg_{H2}} \right] \cdot q_{H2} \left[\frac{kg_{H2}/a}{kW_{H2,LHV}} \right] \cdot HHV_{ng}$$
(24)

$$c_{ng} = P_{ng} \cdot q_{ng} \tag{25}$$

where q_{ng} is the quantity of natural gas per mass of hydrogen produced and P_{ng} is the natural gas price.

Solid carbon cost: hydrogen and solid carbon are the only products of the pyrolysis reaction. For every kg of hydrogen, 3 kg of solid carbon are generated [7,32]. Equation (26) outlines the calculation for the amount of solid carbon produced per unit of hydrogen. This solid carbon can be disposed of, incurring associated costs, or sold, resulting in associated revenues (refer to Equation (27)).

$$q_{C}\left[\frac{kg_{C}}{kW_{H2,LHV}}\right] = y_{c} \cdot q_{H2}\left[\frac{kg_{H2}}{kW_{H2,LHV} \cdot a}\right]$$
(26)

$$c_{C} \left[\frac{\epsilon}{k W_{H2,LHV}} \right] = q_{C} \cdot c_{C} \left[\frac{\epsilon}{k g_{C}} \right]$$
 (27)

2.3. Transmission and distribution

The delivery of hydrogen can be divided into two conceptual stages, namely transmission and distribution. The delivery of hydrogen in these stages can be carried out using various methods, with the most commonly used being pipelines for both stages. However, shipping is usually preferred for the transmission stage, while truck delivery is typically used for distribution purposes. To examine the different methodological approaches utilized by these delivery modes, the subsequent three subsections provide a detailed overview of each.

2.3.1. Pipelines

Compressed gaseous hydrogen can be transported through pipelines using one of three options: constructing new hydrogen pipelines, retrofitting existing gas networks, or blending with natural gas (which is not analyzed in this study). Prior to injection, hydrogen is compressed to the operating pressure of the pipeline, which typically depends on the size, flowrate, and material of the pipeline. Compression stations are also necessary along the pipeline route to maintain pressure difference for flow driving, as stated by references. [3,33].

Pipeline transportation can serve both transmission and distribution purposes for both onshore and offshore applications. In this tool, the choice between constructing new pipelines or retrofitting existing gas networks is included, and it has an effect on various parameters such as the initial investment. Another choice available in the tool is the selection of pipeline size, which offers options between Small, Medium, and

Large, based on Jens et al.'s classification [34]. Equation (28) describes the $LCOH_{r}$:

$$LCOH_{t} = (a_{\%} + OPEX_{\%}) \cdot CAPEX \left[\frac{\epsilon}{km}\right] \cdot l \cdot \frac{LHV_{H_{2}}}{O_{H_{1}} \cdot CF \cdot 8760h}$$
(28)

Given the high level of uncertainty about future projections, the capital costs for pipelines are assumed to be constant throughout the investigation period. The compression stage is a crucial component in the pipeline evaluation, but its methodology is treated separately in Subsection 2.5.1. Nevertheless, it is known that a compression station is required after a distance $l_{segment}$, which depends on flow pressures and velocities and takes into account critical phenomena such as pipeline erosion and pressure control [33]. The iterative process of determining pressures, velocities, and segment lengths is thoroughly explained in Appendix II.

2.3.2. Shipping

Hydrogen shipping can be achieved in liquefied form (as in the case of natural gas), or using chemical compounds such as ammonia and liquid organic hydrogen carriers (LOHCs). Besides the economic benefits, shipping hydrogen can enhance the energy security of the importing countries by providing greater diversification and faster response times to changes in providers, which is especially crucial during sudden geopolitical developments. This is in contrast to pipelines, which may have limited options and longer lead times for changes in providers [3].

The tool considers two options for shipping hydrogen: liquid hydrogen (LH $_2$) and ammonia., with NH $_3$ carriers fueled with heavy fuel oil (HFO) and LH $_2$ ones with boil-off gas (Same assumptions as IEA [3]). The LCOH formula for ammonia ships includes only the vessel's CAPEX and fuel costs (Equation (29)), while for LH $_2$, boil-off losses and their cost are considered, with the potential to partially fuel the ship, resulting in fuel savings (Equation (30))

$$LCOH_{t,NH3} = LCOH_{t,vessel} + LCOH_{t,fuel}$$
(29)

$$LCOH_{t,LH2} = LCOH_{t,vessel} + \max(LCOH_{t,fuel}, LCOH_{t,boiloff})$$
 (30)

Looking at the common elements of Equations (29) and (30), the LCOH vessel component can be calculated using Equation (31). The LCOH vessel component (common to both equations) depends on the number of routes per year (rpa), which is determined by the ship velocity ν , the route distance l, and the average time spent in the harbor t_{harbor} (Equation (32)).

$$LCOH_{t,vessel} = \frac{(a_{\%} + OPEX_{\%}) \cdot \frac{CAPEX_{ship}}{Q_{ghip}}}{rpa}$$
(31)

$$rpa = \frac{8760h}{2 \cdot t_{roundtrip}} = \frac{8760h}{2 \cdot \left(\frac{1}{\nu} + t_{harbor}\right)}$$
(32)

The fuel cost (Equation (33)) is based on the propellant used, while the boil-off loss component, only relevant for LH_2 shipping, is defined by the percentage of boil-off loss, roundtrip time, and the cost of the produced hydrogen being shipped ($LCOH_p$) as described by Equation (34).

$$LCOH_{t,fuel} = \frac{P_{fuel} \cdot E_{fuel} \cdot 2l}{Q_{H2}}$$
(33)

$$LCOH_{t,boiloff} = \frac{b_{\%}}{24h} t_{roundtrip} \cdot LCOH_p$$
 (34)

2.3.3. Truck

The transportation of hydrogen using trucks is a commonly adopted practice. For short distances ($<300\,$ km) compressed gH $_2$ trailers are widely utilized, while LH $_2$ trucks become favorable when the distance

¹ "first-of-a-kind" refers to a new technology or process that has not been implemented before, or that is being implemented for the first time at a large scale. In the context of the Lang factor method, a technology that is first-of-akind is considered to have a higher capital cost than a technology that is "nth-of-a-kind" or more mature, because of the risks associated with implementing a new and unproven technology.

Table 2
Hydrogen storage for different time durations.

	N° of cycles per year	$t_{duration}/t_{cycle}$ [h]	$t_{loading}[h]$
Seasonal storage (1)	1	12 months ⇔ 365 days ⇔ 8760 h	4380
Seasonal storage (2)	2	6 months ⇔ 182 days ⇔ 4380 h	2190
Monthly storage	12	1 month ⇔ 30 days ⇔ 730 h	365
Weekly storage	52	1 week ⇔ 7 days ⇔ 168 h	84
Daily storage	365	1 day ⇔ 24 h	12

offsets the liquefaction costs. Ammonia can be also transported via trucks [3]. The expenses associated with truck transportation are influenced by various factors and can be represented as follows:

atmospheric pressure and a temperature of -33 °C, but may also experience boil-off losses [37,38].

The tool considers gaseous hydrogen as part of the final storage option, and liquid hydrogen or ammonia as intermediate storage options. For storing large quantities of gaseous hydrogen, the tool considers different types of geological reservoirs, namely, salt caverns [39], lined rock caverns [29,40], depleted natural gas or oil reservoirs [41] and aquifers [31,42].

Regardless of the storage option, it is assumed that the OPEX is fixed throughout the economic lifetime of the storage facility, expressed as a percentage of the CAPEX. Equation (2) can be therefore used to assess the $LCOH_s$:

$$LCOH_{s} = \frac{(a_{\%} + OPEX_{\%}) \cdot CAPEX}{Q_{H_{2}}}$$
(39)

$$LCOH_{t,truck} = \frac{CAPEX_{tractor} \cdot a_{\%,tractor} + CAPEX_{tank} \cdot a_{\%,tank} + CAPEX_{tr.chassis} \cdot a_{\%,tr.chassis} + OPEX \cdot l_n}{Q_{H2} \cdot rpa}$$
(36)

$$LCOH_t = LCOH_{t,truck} + LCOH_{t,fuel} + LCOH_{t,driver} + LCOH_{t,boiloff}$$
 (35)

The costs of a vehicle used for hydrogen transportation are calculated by adding the costs of the three truck components: tractor, tank, and trailer chassis. Each of these components has a different lifetime and, therefore, a different amortization factor.

where the *OPEX* is expressed in \in per km, and l_n is the annual distance covered by a truck. As for shipping, the transported capacity Q_{H2} refers to the specific carrier and is hence converted to gaseous hydrogen equivalent mass for the calculations. The routes per year, rpa, are expressed as the ratio between the annual mileage and the average distance per round trip.

The equation for calculating fuel costs is similar to the shipping counterpart (Equation (33)) and is represented by Equation (37):

$$LCOH_{t,fuel} = \frac{P_{fuel} \cdot E_{fuel} \cdot 2l}{Q_{H2}}$$
(37)

Driver costs are explicitly calculated in the truck transportation scenario as they have a significant impact on the Total Cost of Ownership (TCO) and are dependent on the range of the truck.

$$LCOH_{t,driver} = \frac{c_{driver} \cdot t_{op}}{Q_{H2} \cdot rpa}$$
 (38)

where c_{driver} is the driver salary per hour and t_{op} are the annual hours of operation.

Finally, the costs associated with boil-off, which only occur during the transportation of LH_2 , are evaluated using a method similar to that shown in (34).

2.4. Storage

In the tool, hydrogen can be stored in two ways: in storage tanks or in geological reservoirs. In storage tanks, hydrogen can be stored either in gaseous form or in liquid form. When stored as a gas, it is typically stored in tanks at high pressure (up to 700–1000 bar), which can hold different amounts of gas depending on the type of tank and materials used [35, 36]. Liquid hydrogen, on the other hand, is stored in cryogenic tanks at atmospheric pressure, but there may be losses due to boil-off [35,36]. Similarly, ammonia can also be stored in cylindrical tanks at

The annual amount of hydrogen handled Q_{H_2} is:

$$Q_{H_2} = n_{cycles} \cdot Q_{storage} \cdot (1 - m_{losses}) = n_{cycles} \cdot \rho_{H_2} \cdot V_{storage} \cdot (1 - m_{losses})$$
(40)

where $Q_{storage}$ and $V_{storage}$ are the storage capacity, in mass and volume terms. The storage sizing and its CAPEX depend on the form in which hydrogen is stored: Subsection 2.4.1 discusses the gaseous hydrogen storage, while Subsection 2.4.2 covers the liquid hydrogen and ammonia ones.

2.4.1. Gaseous storage

Hydrogen in its gaseous form can be stored in either storage tanks or geological reservoirs. The sizing methodology for both options is similar, but there is a crucial difference - a cushion gas volume must be considered when storing hydrogen in geological reservoirs. The storage sizing depends on two factors, the quantity of hydrogen to be stored and the storage duration. The tool offers five duration options for storage, ranging from short-term to seasonal, as summarized in Table 2. For each duration option, the loading time is assumed to be half of the intended storage duration.

Given the above discussion, the desired storage capacity would therefore be:

$$V_{storage} = V_{working \ gas} + V_{cushion \ gas} = \frac{1}{\rho_{H_2}} \frac{Q_{H_2}}{1 - cushion \ gas_{\%}} \frac{t_{loading}}{8760h}$$
(41)

The cushion gas ratio depends on the geological reservoir typology, while it is set to zero for pressure vessels. For reservoirs, the cost of the cushion gas kept in the reservoir needs to be considered. As such, Equation (39) needs to be adjusted to reflect this additional cost as follows:

$$LCOH_{s} = \frac{(a_{\%} + OPEX_{\%}) \cdot CAPEX + a_{\%} \cdot C_{gas}}{Q_{H_{2}}}$$
(42)

where C_{gas} is the cost of the cushion gas kept in the reservoir:

$$C_{gas} = \rho_{H_2} \cdot V_{cushion \ gas} \cdot P_{H_2} = \frac{Q_{storage}}{1 - cushion \ gas_{\%}} \cdot cushion \ gas_{\%} \cdot P_{H_2}$$
 (43)

with the price of hydrogen P_{H_2} assumed to be the sum of the levelized cost of production and transmission of the selected pathway in the tool.

The CAPEX of gaseous hydrogen storage is calculated considering a scaling effect, following the approach of Reuβ et al. [43] and W. A. Amos

General input		PR	ODUCTION
Select YEAR	Select DESTINATION COUNTRY	Select PRODUCTION LOCATION	Select PRODUCTION METHOD
2030	Germany	Algeria	Electrolysis
			·
CoolProp can be used in the tool to have a better approximation of the		Plant capacity: [kW]	100000
different fluid properties and can be download at the link		Override: [kW]	
Use CoolProp? No			
OBS: To design a new supply pathway, check and select every option (in red) in this table -> Excel does not update the toggle lists!		Select ELECTRICITY SOURCE:	Solar
		Select ELECTROLYZER TYPE:	PEM
		Click here to	change default values

LCOH:	6,3 €/kg	2,09 €/kg
	OVERALL	PRODUCTION

TRANSMISSION			DISTRIBUTION
Select TR. MODE by SEA	Select TR. MODE by LAND		Select DISTR. MODE
Ship	Pipeline		Truck
Select CARRIER	New or repurposed?	H2 carrier selection:	
LH2	New	AUTOMATIC or MANUAL?	New
		AOTOWATIC OF WANDAL!	
Default distance: 3174 km	Default distance: 0 km		Default distance: 200 km
Override below [km]	Override below [km]	Automatic	Override below [km]
Change default values	Change default values		Change default values

3,25 €/kg

TRANSMISSION AND DISTRIBUTION (without int. storage)

STORAGE at IMPORT TERMINAL?	STORAGE at EXPORT TERMINAL?	FINAL STORAGE?	Select H2 FINAL STATE
Yes	Yes	Yes	gH2
Default capacity: 11000 t_LH2	Default capacity: 11000 t_LH2	Default capacity:	Default final pressure: 300 bar
Change default capacity	Change default capacity	Change default capacity	Override below [bar]
		Select STORAGE TYPE	
		Geological - Depleted NG or Oil Reservoir	
		Obs: final storage only as gH2	
Change default values	Change default values	Change default values	

0,11 €/kg	0,82 €/kg	0,02 €/kg
INTERMEDIATE STORAGE	FINAL STORAGE	FINAL CONVERSION

Fig. 3. Snapshot of the top part of the Home sheet in the designed tool.

[44], in which the scaling effect is limited to a maximum design volume.

operating pressures, such as for hydrogen compression before storage or

$$CAPEX = \left| \frac{V_{storage}}{V_{max}} \right| \cdot CAPEX_{ref} \cdot \left(\frac{V_{max}}{V_{ref}} \right)^{sf} + CAPEX_{ref} \cdot \left(\left(\frac{\max(V_{storage}; V_{min})}{V_{max}} - \left\lfloor \frac{V_{storage}}{V_{max}} \right\rfloor \right) \cdot \frac{V_{max}}{V_{ref}} \right)^{sf}$$

$$(44)$$

If the desired quantity to be stored exceeds this upper limit, then multiple tanks $\lfloor V_{storage}/V_{ref} \rfloor$ are required. For geological reservoirs, a minimum amount of hydrogen storage is taken into account, which limits the minimum size of the reservoir. This may result in an oversized storage when the desired quantity of hydrogen is smaller than this lower limit. The general equation used for this calculation is as follows:

2.4.2. Liquid hydrogen and ammonia storages

The storage of liquid hydrogen or ammonia is modeled as a buffer to facilitate the shipping of hydrogen, and can be situated at both the import and export terminals. When storing ammonia, Equation (40) can be formulated as follows:

$$Q_{H_2} = \frac{m_{H_2}}{m_{NH_3}} \cdot \left(n_{\text{cycles}}\right)_j \cdot Q_{\text{storage},NH_3} \cdot (1 - m_{\text{losses}})$$

$$\tag{45}$$

where m_{H_2}/m_{NH_3} is the percentage of hydrogen present in ammonia,

transportation via truck, and multi-stage centrifugal compressors for stable flow conditions, higher flow rates, and lower pressure requirements, such as in pipeline [47].

To assess the compressor CAPEX, the tool used the scaling factor. In this case, both size and pressure scaling factors characterize the system. This method follows the work of Lahnaoui et al. [10] and W. A. Amos [44]. The compressor size is characterized by its rated power, with a maximum value imposed. If the required rated power is higher, multiple parallel compressors are used.

$$CAPEX = CAPEX_{ref} \cdot \left[\frac{P}{P_{max}} \right] \cdot \left(\frac{P_{max}}{P_{ref}} \right)^{sf} \cdot \left(\frac{p}{p_{ref}} \right)^{sf'} + CAPEX_{ref} \cdot \left(\left(\frac{P}{P_{max}} - \left\lfloor \frac{P}{P_{max}} \right\rfloor \right) \cdot \frac{P_{max}}{P_{ref}} \right)^{sf} \cdot \left(\frac{p}{p_{ref}} \right)^{sf'}$$
(50)

where P and p are respectively the system rated power and pressure; sf is the size scaling factor; sf' is the pressure scaling factor.

$$CAPEX = CAPEX_{ref} \cdot \left| \frac{V_{storage}}{V_{max}} \right| \cdot \left(\frac{V_{max}}{V_{ref}} \right)^{sf} + CAPEX_{ref} \cdot \left(\left(\frac{V_{storage}}{V_{max}} - \left| \frac{V_{storage}}{V_{max}} \right| \right) \cdot \frac{V_{max}}{V_{ref}} \right)^{sf}$$

$$(47)$$

equal to 17.65% [45]. For both liquid hydrogen and ammonia, the mass losses are directly linked to the liquid carrier boil-off losses, $b_{\%}$:

$$m_{losses,\%} = b_{\%} \left[\% / day \right] \cdot t_{storage} \left[days \right]$$
 (46)

The CAPEX calculations follow an approach similar to the gaseous storage case:

2.5. Conversion

Hydrogen conversion is used in this paper as a broad term that encompasses hydrogen compression, liquefaction, regassification, and conversion from and to ammonia. For simplification, continuous operations are assumed for almost every case, so that the quantity of converted hydrogen is equal to:

$$Q_{H_2} = availability_{\%} \cdot 8760h \cdot \dot{Q}_{H_2} \cdot (1 - m_{losses})$$

$$\tag{48}$$

where \dot{Q}_{H_2} is the constant hydrogen flowrate to be converted. The compression of gaseous hydrogen for storage applications has a more cyclical nature (loading and unloading phases), so in that case Q_{H_2} is described with Equation (49):

$$Q_{H_2} = t_{loading} \cdot n_{cycles} \cdot \dot{Q}_{H_2} \cdot (1 - m_{losses})$$
(49)

2.5.1. Compression

A compression stage involves increasing the pressure of a gas, and it is a critical step that depends on the flow rate capacity and required compression ratio [46]. These factors also determine the type of compressor technology that should be used. The tool considers two compressor types: multi-stage reciprocating compressors for high

Variable and fixed OPEX are also important components of the compression component of LCOH. Fixed OPEX are calculated as a percentage of the CAPEX, while variable OPEX are dependent on the electrical consumption of the system. For transportation purposes, the system's availability is assumed to be continuous, and as such, the annual electricity consumption E_{el} is influenced by an availability factor:

$$E_{el} = P \cdot availability_{\%} \cdot 8760h \tag{51}$$

For storage options, cyclical operations are considered, therefore the electricity consumption depends on their frequency, i.e., the number of cycles:

$$E_{el} = P \cdot t_{loading} \cdot n_{cycles} \tag{52}$$

The desired rated power P eventually depends on a wide array of factors, such as the hydrogen flow rate and the system efficiencies, pressures, and temperatures. A detailed explanation of this variable can be found in Appendix III.

2.5.2. Conversion from and to liquid hydrogen and ammonia

This subsection describes the conversion of gaseous hydrogen from and to its liquid form, as well as from and to ammonia. Hydrogen liquefaction is a complex process that involves multiple stages of compression, cooling, and expansion, resulting in a phase change from

Table 3Parameters studied for each stage of the hydrogen supply chain.

	Production	T&D	Storage
Varying parameters	Year Size Fuel price	Distance	Size Duration

Table 4Summary of supply pathway options.

Supply pathway		1	2	3	4
Description		Centralized, large-scale PV electrolysis from remote location	Distributed, small-scale PV electrolysis	Centralized, large-scale SMR with CCS	Small-scale pyrolysis
Production	Method	Electrolysis + PV	Electrolysis + PV	SMR with CCS	Pyrolysis
	Capacity [MW]	100	1	300	10
Transmission	Method &	a. New, offshore pipeline	_	Onshore pipeline	-
	Carrier	b. LH ₂ shipping			
	Distance [km]	2000	0	300	0
Storage	Type	Geological	Tank	Geological	Tank
	Duration	Monthly	Daily	Monthly	Weekly
Distribution	Method &	a. Pipeline	_	Pipeline	a. Pipeline
	Carrier	b. LH ₂ truck			b. gH ₂ truck
	Distance [km]	100	0	100	100

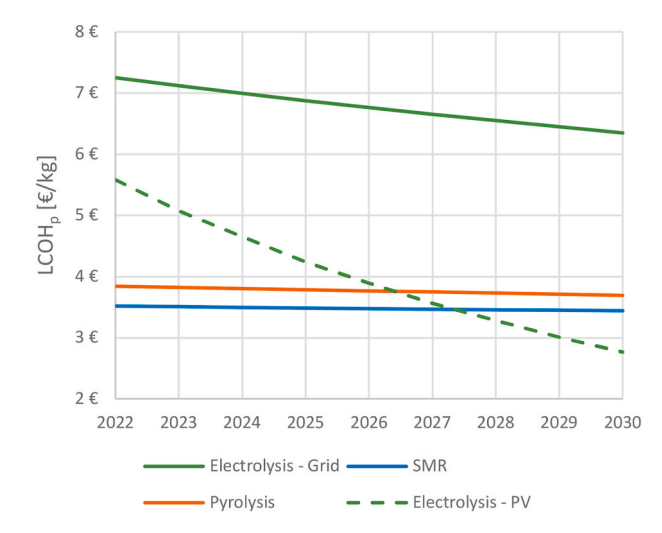


Fig. 4. Levelized cost of hydrogen production, impact of learning effects.

gas to liquid at a temperature below -253° [48]. Among several liquefaction processes, the tool considers only the Claude process due to its prevalence in industrial applications [49–51].

Regasification is the opposite process of hydrogen liquefaction and involves heating liquid hydrogen above its boiling point to convert it back to a gaseous state [52]. The tool includes the regasification process using a thermal resistance approach, which is often overlooked despite its importance [52].

Ammonia conversion, also known as ammonia synthesis, is the process of producing ammonia by combining hydrogen and nitrogen through the Haber-Bosch (H–B) process [3,53]. The reverse process, ammonia cracking, is an endothermic reaction in which ammonia is cracked into hydrogen and nitrogen at very high temperatures [45].

Generally describing the costs of a conversion plant, its CAPEX depends on its capacity $Q_{carrier}$ and an installation factor f_{in} :

$$CAPEX = f_{in} \cdot CAPEX_{ref} \cdot \left(\frac{Q_{carrier}}{Q_{ref}}\right)^{sf}$$
(53)

The ammonia conversion CAPEX is given by the sum of its two main components, the Haber-Bosch stage and the air-separation unit required to obtain nitrogen. The plant capacity $Q_{carrier}$ is expressed in kg of hydrogen for liquefaction and regasification, and in kg of ammonia for its conversion and reconversion stages. Their relationship is defined by the hydrogen mass content in ammonia, m_{H_2}/m_{NH_3} .

Variable and fixed OPEX are also an important component of the compression LCOH. The fixed OPEX is calculated as a percentage of the CAPEX while the variable OPEX is rather based on the system electrical consumption:

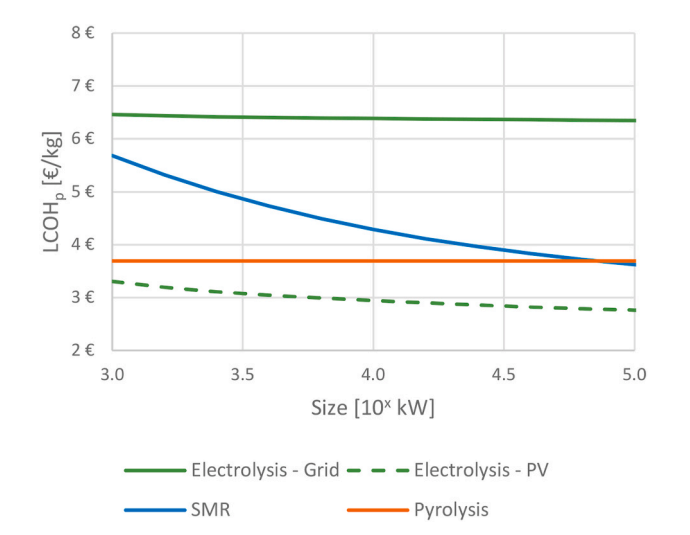


Fig. 5. Levelized cost of hydrogen production, impact of scaling effects in 2030.

$$E_{el} = \left(\sum_{stages} SEC_i\right) \cdot Q_{carrier} \cdot availability_{\%} \cdot 8760h \tag{54}$$

where SEC is the specific energy consumption for each stage in $kWh_{el}/kg_{carrier}$. The SEC is a constant value with the exception of liquefaction, where a dependence on the plant size has been observed. Therefore, an empirical function has been extrapolated to describe the relationship, based on respective values in the literature [54–56]. If the plant's size is larger than a size Q_{max} , the liquefaction SEC also becomes constant [52].

$$SEC = \begin{cases} 17.124 \cdot Q_{carrier}^{-0.216} & Q_{carrier} < Q_{max} \\ SEC_{max} & Q_{carrier} \ge Q_{max} \end{cases}$$
 (55)

2.6. The tool

The central element of this research is the development of a tool that gathers the LCOH calculations for each stage and combine them together to assess the LCOH of a chosen supply pathway. The designed tool is a general model, valid for any location, option, and year. At the current moment, the tool covers specific countries, and the temporal scale is limited, and a predetermined set of values is proposed. However, a user has the total freedom to override any value and to extend the geographical and temporal scope of the tool, which is facilitated by the tool being a user-friendly platform. To provide a general outline, this article uses a *generic country* as production and destination locations.

The Home sheet of the tool gives the possibility to select different

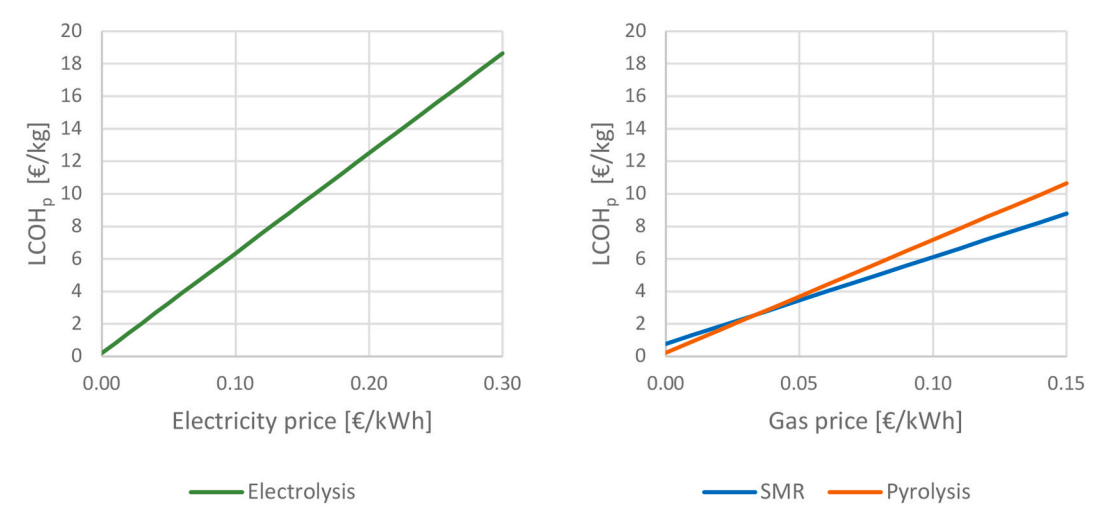


Fig. 6. Levelized cost of hydrogen production, impact of fuel prices in 2030.

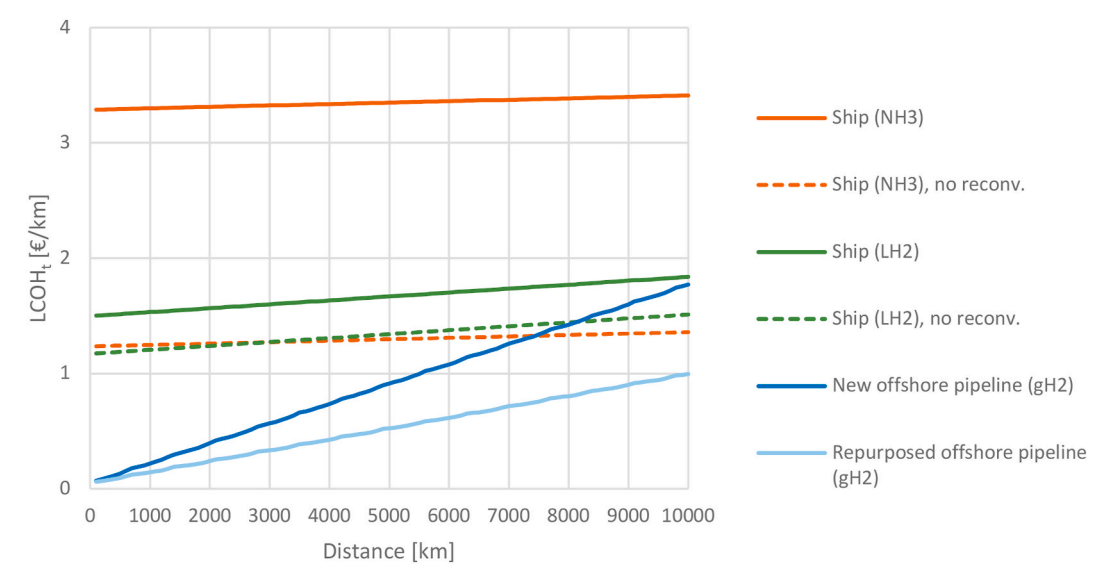


Fig. 7. Levelized cost of hydrogen transmission, impact of distance in 2030.

options for production, T&D, and storage technologies. Fig. 3 shows a screenshot of the top part of the *Home* sheet. The *Home* sheet is the main interface of the tool, and it is linked to several other sheets that encompasses the respective calculations for each stage. Those calculation sheets are fully accessible by users who further have the freedom to override the default input values.

2.7. Supply pathways

Two assessments are carried out to study the functionalities of the tool and assess the results. The first assessment involves the analysis of the impact of individual parameters on the LCOH for each stage of the hydrogen supply chain. Table 3 summarizes the parameters studied for each stage.

The second assessment involves the definition of several supply pathways for a generic country, which is used as an example to calculate the LCOH for the entire hydrogen supply chain. For this assessment, the reference year is 2030 and literature values are used, with global averages being used where possible, and European averages being used in cases where the data varied greatly among regions. The final state in this assessment was gaseous hydrogen at 300 bar.

Four supply pathways were defined and analyzed. The first two

pathways involved electrolysis powered by a dedicated PV plant, with one representing a centralized, large-scale case where delivery is carried out from a remote location via pipeline or shipping, and the security of supply is ensured by geological storage. The other pathway represents a distributed, small-scale case located close to the final consumption.

The other two pathways involved: one with SMR and CCS, that suggests a centralized, large-scale plant; another with hydrogen produced through pyrolysis, representing a smaller plant located closer to the final use. Table 4 reports the supply pathways that were analyzed and their main assumptions. The detailed settings for each supply pathway can be found in Appendix IV, with both their numeric assumption and source.

3. Results

This section provides an exposition of the tool's functionality and its outcomes. In subsections 3.1, 3.2, and 3.3, the results for individual stages are presented, focusing on the analysis of specific parameters related to production, transmission and distribution, and storage. Additionally, Subsection 3.4 present the results of LCOH for the entire supply chain for the generic supply pathways.

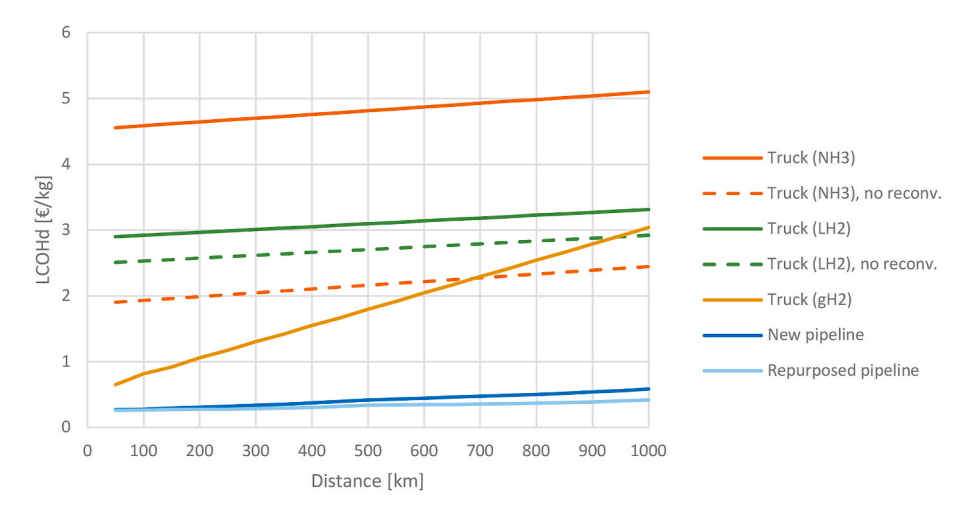


Fig. 8. Levelized cost of hydrogen distribution, impact of distance in 2030.

3.1. Production

The three production methods considered by the tool, namely electrolysis by electricity, SMR, and pyrolysis are investigated. Two configurations of electrolysis: an alkaline electrolyzer connected to the grid and running constantly, and a PEM electrolyzer coupled with a dedicated PV plant are analyzed. For SMR, a single configuration is considered: a plant with CCS and fueled completely by natural gas.

To assess the cost of hydrogen production stage, three elements are considered: learning rates, scaling factors, and the respective fuel prices. Te impact of each factor is presented in the following paragraphs.

First, we examine learning effects, which determine a decrease in CAPEX and subsequently in the LCOH throughout the years. Fig. 4 shows the LCOH_p in different years for each technology, assuming constant grid electricity and gas prices of $0.10~\epsilon/\text{MWh}$ and $0.05~\epsilon/\text{MWh}_{ng,\text{HHV}}$, respectively. Among the three production methods, electrolysis connected to a dedicated PV plant shows the steepest trend, potentially cutting down the LCOH by $2.8~\epsilon/\text{kg}$ by the end of the decade, making green hydrogen the cheapest option by 2028.

The study suggests that green hydrogen, produced by electrolysis powered by photovoltaic can become the most cost effective option by the year 2028. This can be due to the interplay of two different aspects, one is the learning effects that would lead to a decrease in the cost of electrolysis equipment over time, and the other is economies of scale that make large-scale green hydrogen production more efficient.

Second, we take into account the scaling effect, which determines a reduction in CAPEX and LCOH with the upscaling of the production facility. Fig. 5 shows the scaling effects in LCOH for each option in 2030, with SMR being a competitive technology only at large scales, while the other options are less influenced due to their more modular anature.

Last, the respective fuel prices are also an important component for the $LCOH_p$, as clearly shown in Fig. 6. The impact is linear in all three production cases. For electrolysis, constant increase of $0.6~\epsilon/kg$ per every additional ϵ/kWh is observed. Pyrolysis has shown to be more sensitive than SMR to gas prices with an additional $\epsilon/kWh_{ng,HHV}$ causing an increase of $0.7~\epsilon/kg$ for the former, of $0.5~\epsilon/kg$ for the latter.

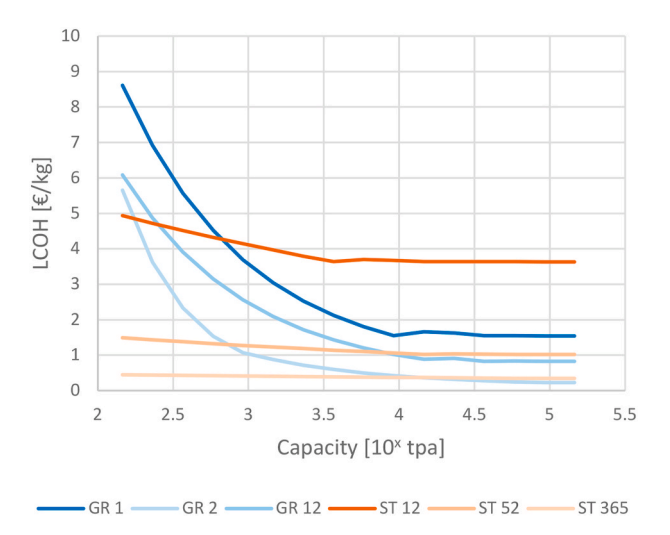


Fig. 9. Levelized cost of hydrogen storage, impact of storage size and duration in 2030.

3.2. Transmission and distribution

The efficient delivery of hydrogen is a crucial aspect in the establishment of a hydrogen global market. The distance between supply and demand determines transportation costs and which delivery method is feasible. Fig. 7 illustrates the relationship between the cost of different transmission modes and their respective distances, considering various transportation means, conversion stages, intermediate storage, and a final state of gaseous hydrogen at 300 bar. Despite the high initial investment for shipping, it does not heavily depend on the distance, resulting in a flatter trend. On the other hand, pipeline³ costs have a closer dependence on the distance, resulting in a steeper variation: for every 1000 km, the LCOH_t via new pipelines increases by approximately 0.18 €/kg, whereas via repurposed pipelines, it increases by about 0.10 €/kg. When considering gaseous hydrogen as the final state of use, repurposed pipelines below 10,000 km are always the cheapest option, while LH₂ becomes competitive with new pipeline infrastructure around 10,000 km. However, NH $_3$ shipping is not economically feasible if gH $_2$ is the desired final state, as its reconversion has a significant impact on ammonia shipping, adding 2.1 €/kg and almost tripling its LCOH_t. If the

² Refers to the ability to easily scale up or down the production capacity. For example, electrolysis can be easily scaled up or down by adding or removing individual electrolyzer units. On the other hand, SMR requires a larger and more complex production facility, which makes it (less modular) more difficult to scale up or down.

 $^{^3}$ Only the offshore infrastructure is shown as it has a similar LCOH to the onshore one with only around a 1% difference despite a 25% higher CAPEX.

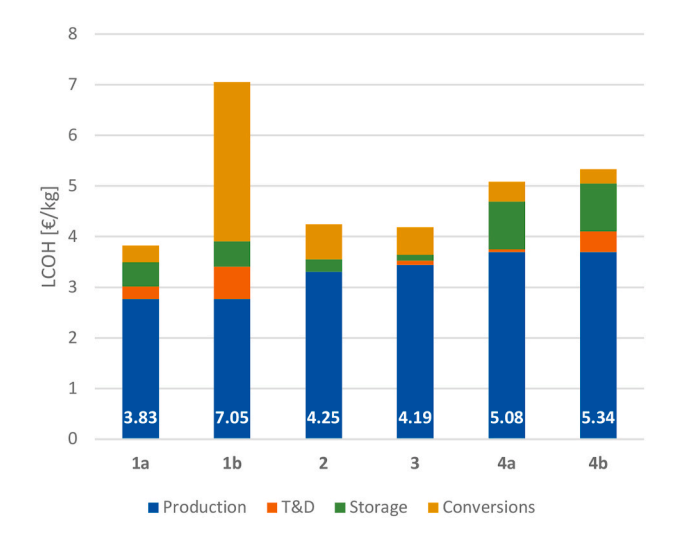


Fig. 10. Levelized cost of hydrogen of the 4 + 2 considered supply pathways.

final state is the same as the delivery one (i.e., no reconversion), NH_3 shipping has similar results to LH_2 shipping.

Similar to transmission, Fig. 8 presents an assessment for the distribution segment, comparing new and repurposed pipelines in their small and medium sizes (respectively, 500 and 900 mm) with truck delivery using three different carriers: gH2 (250 bar), LH2, and NH3. Small size pipelines are limited to a maximum distance of 200 km, following Jens et al. [34] assumptions. In the distance range considered, our results indicate that pipelines are always the cheapest distribution mode. The difference between small and medium pipelines is limited with the medium option has a cost 0.02–0.07 €/kg lower than the smaller one. Despite a steeper trend, gH2 delivery demonstrated to the cheapest option for truck delivery when the final use is gaseous. LH2 transportation costs are somewhat close to gaseous transportation costs, but ammonia costs are very high compared to them, requiring very expensive reconversion at the final point of use. However, when reconversion to gaseous hydrogen is not considered, NH₃ distribution (direct use) appear to be more cost-effective than liquid hydrogen, and even cheaper than gaseous hydrogen for distances greater than 700 km.

3.3. Storage

Hydrogen storage is also a critical element in the realization of a hydrogen-based economy. Its development would facilitate the decoupling of supply and demand and bolster energy security. The size and duration of hydrogen storage, as well as their associated costs, are vital determinants of various supply pathways. Fig. 9 provides a comparison between geological reservoirs (GR), with different numbers of annual cycles (biannual, seasonal, monthly); and storage tanks (ST), with short storage durations (monthly, weekly, daily). A general trend observed is that shorter storage durations result in lower costs. This is because a shorter storage duration allows for a higher number of cycles (i.e., the number of times hydrogen can be stored and retrieved) in the same storage facility, which helps to accelerate the amortization of costs associated with building and maintaining the facility. In other words, more cycles in a shorter time period allows for a quicker return on investment and lower overall costs.

A noticeable trend is that shorter storage durations generally result in lower costs due to the greater number of cycles and hydrogen stored in a single facility, hastening the amortization of costs. However, the relationship between duration and cost should also consider other system needs, such as the security of supply, but optimizing this relationship is beyond the scope of this work. Similarly, the size of storage should be determined with a more systematic view. Nonetheless, it is observed that geological storage only reaches an LCOH_S of around 1

€/kg with sizes greater than 1 Mtpa, and thereafter, the cost curve flattens. Due to their size limitations, storage tanks exhibit a low-cost dependency on size, resulting in a more modular design. They display low LCOH $_{\rm s}$ only with very short durations, whereas a monthly configuration is only competitive with its geological alternative at small sizes, approximately 100 tpa, but is otherwise very costly. However, the relationship between duration and cost should also consider other system needs, such as the security of supply, but optimizing this relationship is beyond the scope of this work. Similarly, the size of storage should be determined with a more systematic view.

3.4. Overall supply chain

Four supply pathways, with two variations, have been introduced to study the potential of the tool as discussed before. They contrapose large-scale and small-scale; centralized, remote, and distributed; electricity-fueled and gas-fueled cases. The results for 2030 are presented in Fig. 10. Electrolysis powered by PVs (1a) in a remote location has the lowest LCOH when delivered to the end-use region via pipeline, at 3.8 €/kg. 1b scenario was found to be uncompetitive mainly due to high conversion costs to and from LH2. The distributed electrolysis case (2) was 0.4 €/kg more expensive than 1a, despite requiring no delivery and smaller storage, which can be attributed to the smaller scale of the configuration. SMR with CCS (4) had similar costs due again to a more expensive production stage which dampen the upscaling advantages in the storage and delivery phases. Finally, pyrolysis scenario (4) represented by the last two pathways, was the second most expensive case owing to the small scale and high storage costs. Pipeline distribution (4a) was found to be 0.3 €/kg cheaper than its gaseous hydrogen respective (4b).

These results might appear higher than other literature and industrial projections. For example, the LCOH values calculated in a report by Lazard lies in the range of \$1.68-\$4.28 when there is subsidy and can go up to \$4.77-\$7.73 without subsidy for green hydrogen [57]. The values are further lower for pink hydrogen. However, it is worth mentioning again that these pathways consider average input values. Therefore, the hydrogen cost can be largely cheaper when considering location with exceptional conditions, such as large RES availability or low gas prices. These favorable locations cannot be neglected, since they potentially correspond to the first sites where hydrogen projects will be developed. The tool provides a significant advantage in that regard by enabling users to input location- and case-specific values and promptly obtain the LCOH for a given supply chain.

On the other hand, the analysis of hydrogen production methods reveals the potential for notable cost reductions through learning effects and scaling factors, particularly evident in electrolysis configurations integrated with dedicated PV plants. Furthermore, the examination of transport and distribution indicates that repurposed pipelines and gaseous hydrogen delivery offer competitive advantages over alternative methods for certain distances. This in turn highlights the importance of considering distance and delivery methods in optimizing cost efficiency. For storing hydrogen, our evaluation points out the importance of storage duration and capacity in managing costs. Shorter storage periods result in lower costs due to more frequent cycling, which stresses the need for an optimum storage design that considers economic and operational factors.

4. Conclusion

This study introduces a tool that can be used to assess the levelized cost of a hydrogen supply chain. The main objective of this research is to share a complete methodology, which encompasses all stages of the hydrogen supply chain, enabling a holistic view on the topic. This also corresponds to the novelty of the study, which proposes to go beyond the separate analysis of each individual stage and instead combine them in a sole body of work. By examining the different stages of the supply chain

(production, transmission and distribution, and storage), we have identified key drivers that can lead to a decline in hydrogen costs in the near future.

Economy of scale is one of the most important factors that can lead to a decrease in hydrogen costs. This effect can result from both technological learning and capacity upscaling. The learning effect is particularly important for electrolysis, especially when coupled with RES, with a potential cost decrease of 2–3 ℓ /kg from 2022 to 2030. Capacity upscaling benefits both production and storage. For the former, it confirms the large-scale nature of SMR, and it suggests a potential decrease with the upscaling of electrolyzer-PV systems. For the latter, geological reservoirs are particularly influenced by the scaling effect, verifying also in this case a more favorable inclination for large capacity sites. In contrast, storage tanks are not much affected by upscaling due to their modular nature.

Another key driver of hydrogen costs is the price of input fuels, such as electricity or gas. Low electricity costs, particularly for electrolysis-RES systems, could make green hydrogen more competitive in the market. Finally, the distance between supply and demand can define preferred methods and enable supply from remote locations, which could also impact costs.

Some generic supply pathways were considered for hydrogen with combination of different options and technologies for each stage to impart a deeper understanding of the functionalities of the tool. The considered supply pathways also provide a clear indication that, where available, pipelines are the best option for both transmission and distribution. This is due to the high costs associated with the conversion and compression stages required for shipping and truck delivery, which make these options less feasible.

While the present study offers an initial comparison of diverse alternatives and supply pathways, certain limitations are noted, such as the use of generic literature values that are not specific to any location. However, we believe that hydrogen projects will be situated in highly advantageous areas, particularly during the early stages of hydrogen economy.

Given the number of options provided in this multi-option analytical tool, it provides immense possibilities to design various innovative pathways through combinations of these options, which can provide novel insights if different pathways are chosen. Further, the tool is simple to use, it is replicable as well as scalable which means it can be expanded to other locations if updated with additional dataset. Thereby,

the tool contains scientific vigor and background of whole hydrogen supply chain, which can be used analysis of various test cases. The flexibility of the tool to add additional technologies further makes it valuable for assessing hydrogen growth pathways. Such observations can support policy makers to tailor their efforts towards specefic region or technology while maximizing the efficiency and effictiveness of hydrogen deployment efforts.

Further, this comprehensive evaluation of different stages of the hydrogen supply chain gives a holistic understanding of the cost dynamics thereby aiding in designing strategic pathways. In addition, the tool considers multiple factors like learning rates, scaling effects, fuel prices and future prognosis methodology. These factors can, therefore, help policymakers to make informed decisions in terms of prioritizing and designing investment pathways as well as policy interventions to promote uptake of hydrogen economy.

CRediT authorship contribution statement

Pietro Dogliani: Conceptualization, Data curation, Formal analysis, Methodology, Validation, Visualization, Writing – original draft, Writing – review & editing. Afonso Nolan Ruas Rego Canha: Conceptualization, Data curation, Formal analysis, Methodology, Visualization, Writing – original draft, Writing – review & editing. Ahmed M. Elberry: Formal analysis, Investigation, Methodology, Supervision, Validation, Writing – original draft, Writing – review & editing. Jagruti Thakur: Conceptualization, Investigation, Methodology, Project administration, Resources, Supervision, Validation, Writing – review & editing.

Declaration of competing interest

The authors declare that they have no known competing financial interests or personal relationships that could have appeared to influence the work reported in this paper.

Data availability

The tool can be found at https://github.com/jagruti-T/Multi-Option-Analytical-Modeling-of-Levelized-Costs-Across-Various-Hydrogen-Sup ply-Chain-Nodes.git.

Appendix I. Electrolysis parameters

This section provides more details about some key parameters introduced in Section 2.2.1.

CAPEX, scaling and sizing factor: The costs for an electrolyzer can be broken down in stack and other costs. The other costs, from now referred as auxiliary costs, include power electronics, gas conditioning, and balance of plant. Learning and scaling effects are considered and, to add some levels of detail, they are determined at a component level, dividing the electrolyzer system in stack and auxiliary components. Accounting for stack and other components independently, Equation xx can be rewritten as:

$$c(t) = c_0 \cdot \left[\%_{st2tot,0} \cdot (1 + AGR)^{-b_{st}(t-t_0)} + \left(1 - \%_{st2tot,0} \right) \cdot (1 + AGR)^{-b_{aux}(t-t_0)} \right]$$
(56)

where %_{st2tot.0} is the ratio between the stack and the total electrolyzer system cost in 2021.

The scaling effects are also taken into account, meaning that a larger electrolyzer system has a lower CAPEX per unit of capacity [24]. This analysis usually refers to specific costs (ℓ/kW_{el}), therefore from Equation (7):

$$c = \frac{C}{S} = \frac{1}{S} \cdot \left[C_{ref} \cdot \left(\frac{S}{S_{ref}} \right)^{sf} \right] = \frac{1}{S} \cdot \left[\left(S_{ref} \cdot c_{ref} \right) \cdot \left(\frac{S}{S_{ref}} \right)^{sf} \right] = c_{ref} \cdot \left(\frac{S}{S_{ref}} \right)^{sf-1}$$

$$(57)$$

The scaling factor *sf* is specific to each component since the impact of the upscaling on the costs depends on the design and the structure of each component. Following the same approach used for the learning curves, where the electrolyzer is divided in two parts, stack and auxiliary components, Equation (57) can be rewritten as:

P. Dogliani et al.

$$c_{el} = c_{ref} \cdot \left[\%_{st2sys} \cdot \left(\frac{S}{S_{ref}} \right)^{sf_{st}-1} + \left(1 - \%_{st2sys} \right) \cdot \left(\frac{S}{S_{ref}} \right)^{sf_{aux}-1} \right]$$

$$(58)$$

The electrolyzer stack has a modular design that prevents a large cost reduction due to its upscaling. In fact, the single cell is limited in size for different reasons (e.g., issues with leakage), with the maximum cell stack size expected to slightly increase thanks to learning effects [24]. Zauner et al. [24] use a dynamic scaling factor for the cell stack, that depends on the system size, and thus minimizes the scaling effects for large-scale applications:

$$sf_{st} = 1 - \left(1 - sf_{st,0}\right) \cdot e^{-\frac{S}{S_{max}}} \tag{59}$$

where $sf_{st,0}$ is the basic scaling factor and S_{max} is the average maximum stack size. For auxiliary components, the scaling effect does not consider a maximum facility size. However, due to the nature of the formula, little variations are noticed for very large system sizes. Therefore, additional corrections are disregarded with the proposed formula.

The combination of learning and scaling effects is considered in the tool, where the system CAPEX can be obtained for a determined year and size, knowing the CAPEX for a 1 MW_{el} system in 2021. The general formula used in the tool is here reported, describing both learning and scaling effects by combining Equations (56), (58) and (59).

$$c_{el} = c_{ref} \cdot \left[\%_{st2sys} \cdot (1 + AGR)^{-(t-t_0) \cdot \log_2(1-LR_{st})} \cdot \left(\frac{S}{S_{ref}} \right)^{(1-sf_{st,0}) \cdot e^{-s/S_{max}}} + \left(1 - \%_{st2sys} \right) \cdot (1 + AGR)^{-(t-t_0) \cdot \log_2(1-LR_{stux})} \cdot \left(\frac{S}{S_{ref}} \right)^{sf_{aux}-1} \right]$$

$$(60)$$

Efficiency: The electrolyzer stack is subject to degradation, therefore this effect needs to be considered as a time-relevant decrease in efficiency [58]. Assuming that the efficiency degrades linearly during its lifetime, the average efficiency in a year n is equal to:

$$\eta_{el,n} = \eta_{el,0} - D_{\eta} \cdot \frac{\overline{h_n}}{IT} = \eta_{el,0} - D_{\eta} \cdot \frac{(h_n + h_{n-1})/2}{IT}$$
(61)

where $\eta_{el,0}$ is the nominal stack electrical efficiency; D_{η} is the lifetime efficiency degradation; $\overline{h_n}$ is the cumulative average hours of use in year n; LT is the stack lifetime. The annual hydrogen production thus decreases with an increasing number of hours of use of the stack.

Levelized cost of electricity: The concept of LCOE has been introduced previously to describe the LCOH. However, a more detailed explanation is needed since the LCOE is explicitly used and calculated in the tool. Similarly to Equation (2), the LCOE can be expressed as:

$$LCOE = \frac{(a_{\%} + OPEX_{\%}) \cdot CAPEX_{t}}{E.}$$
(62)

where E_t is the annual energy generated, assumed to be constant throughout the lifetime of the system [21]. If $CAPEX_t$ and E_t refer to a single unit of capacity, Equation (62) can be rewritten as:

$$LCOE = \frac{(a_{\%} + OPEX_{\%}) \cdot CAPEX}{CF \cdot 8760h}$$
(63)

where CF is the RES capacity factor.

Appendix II. Fluid dynamics in pipelines

To allow for a safe and efficient transportation in pipelines, hydrogen needs to be compressed in compression stations along its route. The distance between two consecutive stations, also referred as segment length, is the result of an iterative process based on Khan et al. [33]. The calculations also provide the pressure value at the end of the pipeline segment, p_{out} , that corresponds to the input pressure for the next booster compressor:

$$p_{out} = \left[p_{op}^2 - G \cdot T_f \cdot l_{segment} \cdot Z \cdot f \cdot \left(\frac{Q_{H2}}{K \cdot D^{2.5}} \cdot \frac{P_b}{T_b} \right)^2 \right]^{0.5}$$

$$(64)$$

where G is the hydrogen specific gravity (0.0696, dimensionless quantity); T_f is the average flow temperature; Z is the compressibility factor, approximated to be equivalent to the one at base pressure and temperature (1.031, dimensionless quantity); K is an equation constant (0.0011494, dimensionless quantity); P_b and T_b are the base pressure (101.352 kPa) and temperature (288.706 K); f is the friction factor, calculated from the Haaland equation that is shown hereby:

$$\frac{1}{\sqrt{f}} = -1.8 \cdot \log_{10} \left(\left(\frac{\varepsilon}{3.7 \cdot D} \right)^{1.11} + \frac{6.9}{Re} \right) \tag{65}$$

where ε is the pipeline roughness and Re is the flow average Reynolds number. The Reynolds number also depends on the velocity, that can be calculated as follows:

$$v = 14.734 \cdot \frac{P_b}{T_b} \cdot \frac{Z \cdot T}{p} \cdot \frac{Q}{D^2}$$
 (66)

Equation (66) is dependent on the pressure, and therefore also the friction factor (Equation (65)), explaining the iterative nature of Equation (64). To avoid pipe erosion, the velocity needs to be maintained below a limit erosional velocity:

$$v_{max} = 100 \cdot \sqrt{0.05131 \cdot \frac{Z \cdot R \cdot T_f}{G \cdot p_{op}}}$$

$$(67)$$

The tool ensures that the velocity is always below this limit value by controlling the segment outlet pressure p_{out} (minimum pressure in the pipe segment) to be always higher than the minimum value p_{min} , from Equation (148):

$$p_{min} = 14.734 \frac{P_b}{T_b} \frac{Z \cdot T}{v_{max}} \frac{Q}{D^2}$$
 (68)

Appendix III. Compression rated power

The electricity consumption of a compressor is closely linked to its rated power *P*:

$$P = \frac{P_{real}}{\eta_{electric \ motor}} = \frac{P_{is}}{\eta_{isentropic}} \cdot \frac{1}{\eta_{electric \ motor}}$$

$$(69)$$

where.

- P_{real} is the mechanical power required by the compression station
- $\eta_{electric\ motor}$ is the compressor's electric motor efficiency.
- $\eta_{isentropic}$ is the isentropic efficiency, which varies depending on the compressor technology.
- P_{is} is the isentropic power required by the compression station, described with Equation (70) [59–62].

$$P_{is} = N_{stages} \cdot \left(\frac{k}{k-1}\right) \cdot Z \cdot T_1 \cdot Q_{compr} \cdot R \cdot \left[\left(\frac{p_2}{p_1}\right)^{\left(\frac{k-1}{N_{stages} \cdot k}\right)} - 1 \right]$$

$$(70)$$

where.

- N_{stages} is the number of compressor stages
- k is the heat capacity ratio or isentropic expansion factor
- Z is the gas compressibility factor
- T_1 is the temperature of the feed gas flow.
- Q_{compr} is the mass flow rate of the gas flowing through the compressor
- R is the universal gas constant
- p_1 and p_2 are respectively the pressure of the gas entering and exiting the compressor

The compressibility factor is calculated using the average pressure between inlet and outlet pressures (p_{avg}) and the average temperature between inlet and outlet temperatures (T_{avg}):

$$p_{\text{avg}} = \frac{2}{3} \left(\frac{p_2^3 - p_1^3}{p_2^3 - p_1^2} \right) \tag{71}$$

$$T_{\text{avg}} = \frac{T_1 + T_2}{2}$$
 (72)

where the temperature of the discharge gas flow T_2 is calculated as follows:

$$T_{2} = T_{1} \cdot \left[1 + \frac{\left(\frac{p_{2}}{p_{1}}\right)^{\left(\frac{k-1}{N_{starger} \cdot k}\right)} - 1}{\eta_{isentropic}} \right]$$

$$(73)$$

The number of compressor stages is equal to:

$$N_{stages} = ROUNDUP \left(\frac{log\left(\frac{p_2}{p_1}\right)}{log(x)} \right)$$
(74)

where x is the compression ratio for each stage.

Appendix IV. Supply pathway settings

This section gathers the settings and assumptions for each one of the four proposed supply pathways. All assumptions related to costs and prices are presented in a range, which corresponds to the expected values within the tool horizon (2022–2030). More information on settings and assumptions can be directly found in the tool.

Table 5 lists the settings for the production stage of the first supply pathway.

Table 5
Main settings and assumptions for the production stage of supply pathway (1).

Parameter	Value	Unit	Source
Method	Electrolysis + PV		
Capacity	100	[MW]	Own assumption
Electrolyser technology	PEM		
Energy source	Electricity (dedicated PV)		
RES plant capacity	160	[MW]	Own calculations, based on [7]
OPEX (as % of CAPEX)	1.5%	_	[3]
Nominal discount rate	8%	_	Own assumption
Water cost	0	[€/L]	Own assumption
Oxigen price	0	[€/kg]	Own assumption

Table 6 lists the settings for the production stage of the second supply pathway.

Table 6
Main settings and assumptions for the production stage of supply pathway (2).

Parameter	Value	Unit	Source
Method	Electrolysis + PV		
Capacity	1	[MW]	Own assumption
Electrolyser technology	PEM		
Energy source	Electricity (dedicated PV)		
RES plant capacity	1.6	[MW]	Own calculations, based on [7]
OPEX (as % of CAPEX)	1.5%	-	[3]
Nominal discount rate	8%	-	Own assumption
Water cost	0	[€/L]	Own assumption
Oxigen price	0	[€/kg]	Own assumption

Table 7 lists the settings for the production stage of the third supply pathway.

Table 7Main settings and assumptions for the production stage of supply pathway (3).

Parameter	Value	Unit	Source
Method	SMR with CCS		
Capacity	300	[MW]	Own assumption
Energy source	Natural gas (both as fuel and feedstock)		
Fuel input	3.7	[kg _{NG} /kg _{H2}]	[29]
Average fuel cost	28–32	[€/MWh _{NG, HHV}]	Own assumptions
Average ETS price	120–145	[€/t _{CO2}]	[63] (SDS scenario)
CO ₂ T&S cost	30	[€/t _{CO2}]	[64]
OPEX (as % of CAPEX)	3.9%	_	[29]
Nominal discount rate	8%	_	Own assumption
CO ₂ capture rate	90%	[€/L]	[29]

Table 8 lists the settings for the production stage of the fourth supply pathway.

 ${\bf Table~8}\\ {\bf Main~settings~and~assumptions~for~the~production~stage~of~supply~pathway~(4)}.$

Parameter	Value	Unit	Source
Method	Pyrolysis		
Capacity	10	[MW]	Own assumption
Energy source	Natural gas		
Fuel input	4.9	[kg _{NG} /kg _{H2}]	[31]
Average fuel cost	28-32	[€/MWh _{NG, HHV}]	Own assumptions
Solid carbon price	0	[€/kg]	Own assumptions
OPEX (as % of CAPEX)	5%	_	[31]
Nominal discount rate	8%	_	Own assumption

Table 9 shows the main settings for the transmission stage of the first and third supply pathway. Due to their proximity to the final consumption, the second and fourth supply pathway do not account for a transmission stage and they are therefore disregarded in the table.

Table 9Main settings and assumptions for the transmission stage.

Supply pathway	1a	1b	3
Description	New, offshore pipeline	LH2 shipping	Onshore pipeline
Distance [km]	2000	2000	300
Hydrogen state	Gaseous	Liquid	Gaseous
Operating pressure [bar]	80 [34]	_	80 [34]
Design capacity	13 GW _{H2, LHV} [34]	11 kt _{H2} /ship [3]	13 GW _{H2, LHV} [34]
Nominal discount rate	6% [34]	8% [3]	6% [34]

Table 10 shows the main settings of the hydrogen storage for each supply pathway. In line with their storylines, two supply pathways consider a large-scale, long-duration geological storage, with volumes that depend on the production stage. The other two pathways require smaller volumes given the lower volumes and closer distance to the final consumption.

Table 10
Main settings and assumptions for the storage stage.

Supply pathway	1	2	3	3
Туре	Geological	Tank	Geological	Tank
Subtype	Depleted NG or oil reservoir	Pressure vessel	Depleted NG or oil reservoir	Pressure vessel
Duration	Monthly (730 h)	Daily (24h)	Monthly (730 h)	Weekly (168h)
Operating pressure [bar]	150 [6 5]	325 [36]	150 [65]	325 [36]
Nominal discount rate	8%	8%	8%	8%

Table 11 shows the main settings for the three distribution options considered, with a reference to which supply pathway they have been considered in.

 Table 11

 Main settings and assumptions for the distribution stage.

Distribution option	Pipeline	gH ₂ truck	LH ₂ truck
Supply pathway	1a, 3	1b	4
Distance [km]	100	100	100
Operating pressure [bar]	50 [34]	250 [66]	_
Design capacity	1.2 GW _{H2, LHV} [34]	690 kt _{H2} /truck	4300 kt _{H2} /truck
Nominal discount rate	6%	7%	7%

References

- [1] UNFCCC. "The Paris Agreement." [Online], https://unfccc.int/process-and-meetin gs/the-paris-agreement/the-paris-agreement. [Accessed 3 February 2022].
- [2] Hydrogen Council. "Path to hydrogen competitiveness: a cost Perspective hydrogen Council,". https://hydrogencouncil.com/en/. [Accessed 3 February 2022]. https://hydrogencouncil.com/en/path-to-hydrogen-competitiveness-a-co st-perspective/.
- [3] International Energy Agency. "The future of hydrogen," IEA [Online], https://www.iea.org/reports/the-future-of-hydrogen. [Accessed 3 February 2022].
- [4] Kayfeci M, Keçebaş A, Bayat M. Chapter 3 hydrogen production. In: Calise F, D'Accadia MD, Santarelli M, Lanzini A, Ferrero D, editors. Solar hydrogen production. Academic Press; 2019. p. 45–83. https://doi.org/10.1016/B978-0-12-814853-2-00003-5
- [5] Stockl F, Schill W-P, Zerrahn A. Optimal supply chains and power sector benefits of green hydrogen. Sci Rep Dec. 2021;11(1):14191. https://doi.org/10.1038/s41598-021-92511-6
- [6] Almansoori A, Shah N. Design and operation of a future hydrogen supply chain: Snapshot model. Chem Eng Res Des Jun. 2006;84(6):423–38. https://doi.org/ 10.1205/cherd.05193.
- [7] Brändle G, Schönfisch M, Schulte S. Estimating long-term global supply costs for low-carbon hydrogen. Appl Energy Nov. 2021;302:117481. https://doi.org/ 10.1016/j.apenergy.2021.117481.
- [8] Janssen JLLCC, Weeda M, Detz RJ, van der Zwaan B. Country-specific cost projections for renewable hydrogen production through off-grid electricity systems. Appl Energy Mar. 2022;309:118398. https://doi.org/10.1016/j. apenergy.2021.118398.
- [9] Liu H, Almansoori A, Fowler M, Elkamel A. Analysis of Ontario's hydrogen economy demands from hydrogen fuel cell vehicles. Int J Hydrogen Energy Jun. 2012;37(11):8905–16. https://doi.org/10.1016/j.ijhydene.2012.03.029.

- [10] Lahnaoui A, Wulf C, Heinrichs H, Dalmazzone D. Optimizing hydrogen transportation system for mobility via compressed hydrogen trucks. Int J Hydrogen Energy Jul. 2019;44(35):19302–12. https://doi.org/10.1016/j. ijhydene.2018.10.234.
- [11] Ochoa Robles J, Giraud Billoud M, Azzaro-Pantel C, Aguilar-Lasserre AA. Optimal design of a sustainable hydrogen supply chain network: application in an airport ecosystem. ACS Sustainable Chem Eng Nov. 2019;7(21):17587–97. https://doi. org/10.1021/acssuschemeng.9b02620.
- [12] Reuß M, Grube T, Robinius M, Stolten D. A hydrogen supply chain with spatial resolution: comparative analysis of infrastructure technologies in Germany. Appl Energy Aug. 2019;247:438–53. https://doi.org/10.1016/j.apenergy.2019.04.064.
- [13] Green hydrogen for industrial sector decarbonization: costs and impacts on hydrogen economy in Qatar. Comput Chem Eng Feb. 2021;145:107144. https://doi.org/10.1016/j.compchemeng.2020.107144.
- [14] Kim M, Kim J. Optimization model for the design and analysis of an integrated renewable hydrogen supply (IRHS) system: application to Korea's hydrogen economy. Int J Hydrogen Energy Oct. 2016;41(38):16613–26. https://doi.org/ 10.1016/j.ijhydene.2016.07.079.
- [15] Kim M, Kim J. An integrated decision support model for design and operation of a wind-based hydrogen supply system. Int J Hydrogen Energy Feb. 2017;42(7): 3899–915. https://doi.org/10.1016/j.ijhydene.2016.10.129.
- [16] Won W, Kwon H, Han J-H, Kim J. Design and operation of renewable energy sources based hydrogen supply system: technology integration and optimization. Renew Energy Apr. 2017;103:226–38. https://doi.org/10.1016/j. renene.2016.11.038.
- [17] Penev M, Zuboy J, Hunter C. Economic analysis of a high-pressure urban pipeline concept (HyLine) for delivering hydrogen to retail fueling stations. Transport Res Part Transp Environ Dec. 2019;77:92–105. https://doi.org/10.1016/j. trd.2019.10.005.
- [18] Yang C, Ogden JM. Renewable and low carbon hydrogen for California modeling the long term evolution of fuel infrastructure using a quasi-spatial TIMES model.

- Int J Hydrogen Energy Apr. 2013;38(11):4250-65. https://doi.org/10.1016/j.iihydrogen 2013.01.105
- [19] Li L, Manier H, Manier M-A. Integrated optimization model for hydrogen supply chain network design and hydrogen fueling station planning. Comput Chem Eng Mar. 2020;134:106683. https://doi.org/10.1016/j.compchemeng.2019.106683.
- [20] Short W, Packey DJ, Holt T. "A manual for the economic evaluation of energy efficiency and renewable energy technologies,". Golden, CO (United States): National Renewable Energy Lab. (NREL); Mar. 1995. https://doi.org/10.2172/ 35391. NREL/TP-462-5173.
- [21] Branker K, Pathak MJM, Pearce JM. A review of solar photovoltaic levelized cost of electricity. Renew Sustain Energy Rev Dec. 2011;15(9):4470–82. https://doi.org/ 10.1016/j.rser.2011.07.104.
- [22] J. Gräfström and R. Poudineh, "A critical assessment of learning curves for solar and wind power technologies," Oxford Institute for Energy Studies, pp. 5-6, 2021. Accessed: May 13, 2022. [Online]. Available: https://www.oxfordenergy.org/publications/a-critical-assessment-of-learning-curves-for-solar-and-wind-power-technologies/.
- [23] Schoots K, Ferioli F, Kramer GJ, van der Zwaan BCC. Learning curves for hydrogen production technology: an assessment of observed cost reductions. Int J Hydrogen Energy Jun. 2008;33(11):2630–45. https://doi.org/10.1016/j. iibydene 2008 03 011
- [24] Zauner A, Böhm H, Rosenfeld D, Tichler R, Schirrmeister S. Analysis on future technology options and on techno-economic optimization. Store&Go; Feb. 2019 [Online]. Available: https://www.storeandgo.info/fileadmin/downloads/delivera bles_2019/20190801-STOREandGO-D7.7-EIL-Analysis_on_future_technology_opt ions and on techno-economic optimization.pdf. [Accessed 1 April 2022].
- [25] Chi J, Yu H. Water electrolysis based on renewable energy for hydrogen production. Chin J Catal Mar. 2018;39(3):390–4. https://doi.org/10.1016/S1872-2067(17)62040-8
- [26] IRENA. "Green hydrogen cost reduction," IRENA [Online], https://www.irena.or g/publications/2020/Dec/Green-hydrogen-cost-reduction. [Accessed 30 March 2022].
- [27] Beswick RR, Oliveira AM, Yan Y. Does the green hydrogen economy have a water problem? ACS Energy Lett Sep. 2021;6(9):3167–9. https://doi.org/10.1021/ acsenergylett.1c01375.
- [28] Maggio G, Squadrito G, Nicita A. Hydrogen and medical oxygen by renewable energy based electrolysis: a green and economically viable route. Appl Energy Jan. 2022;306:117993. https://doi.org/10.1016/j.apenergy.2021.117993.
- [29] Collodi G, Azzaro G, Ferrari N, Santos S. Techno-economic evaluation of deploying CCS in SMR based merchant H2 production with NG as feedstock and fuel. Energy Proc Jul. 2017;114:2690–712. https://doi.org/10.1016/j.egypro.2017.03.1533.
- [30] J. C., Hamborg ES, van Keulen T, Ramírez A, Turkenburg WC, Faaij APC. Technoeconomic assessment of CO2 capture at steam methane reforming facilities using commercially available technology. Int J Greenh Gas Control Jul. 2012;9:160–71. https://doi.org/10.1016/j.iiggc.2012.02.018.
- [31] Parkinson B, Matthews JW, McConnaughy TB, Upham DC, McFarland EW. Technoeconomic analysis of methane pyrolysis in molten metals: decarbonizing natural gas. Chem Eng Technol 2017;40(6):1022–30. https://doi.org/10.1002/ ceat.201600414.
- [32] Timmerberg S, Kaltschmitt M, Finkbeiner M. Hydrogen and hydrogen-derived fuels through methane decomposition of natural gas – GHG emissions and costs. Energy Convers Manag X Sep. 2020;7:100043. https://doi.org/10.1016/j. ecmx 2020.100043
- [33] Khan M.A., Young C., Layzell D. Technical brief: the techno-economics of hydrogen pipelines. The Transition Accelerator, pp. 12–14, Nov. 2021. [Online]. Available: https://transitionaccelerator.ca/techbrief-techno-economics-hydrogenpipelines/. [Accessed 19 May 2022].
- [34] Jens J, Wang A, van der Leun K, Peters D, Buseman M. "Extending the European hydrogen backbone," [Online], https://gasforclimate2050.eu/sdm_downloads/ex tending-the-european-hydrogen-backbone/. [Accessed 17 March 2022].
- [35] Hassan IA, Ramadan HS, Saleh MA, Hissel D. Hydrogen storage technologies for stationary and mobile applications: review, analysis and perspectives. Renew Sustain Energy Rev Oct. 2021;149:111311. https://doi.org/10.1016/j. rser 2021 111311
- [36] Langmi HW, Engelbrecht N, Modisha PM, Bessarabov D. Chapter 13 hydrogen storage. In: Smolinka T, Garche J, editors. Electrochemical power sources: fundamentals, systems, and applications. Elsevier; 2022. p. 455–86. https://doi. org/10.1016/B978-0-12-819424-9.00006-9.
- [37] Elishav O, Mosevitzky Lis B, Valera-Medina A, Grader GS. Chapter 5 storage and distribution of ammonia. In: Valera-Medina A, Banares-Alcantara R, editors. Techno-economic challenges of green ammonia as an energy vector. Academic Press; 2021. p. 85–103. https://doi.org/10.1016/B978-0-12-820560-0.00005-9.
- [38] Al-Breiki M, Bicer Y. Technical assessment of liquefied natural gas, ammonia and methanol for overseas energy transport based on energy and exergy analyses. Int J Hydrogen Energy Dec. 2020;45(60):34927–37. https://doi.org/10.1016/j. iihydene.2020.04.181.
- [39] Lord AS, Kobos PH, Borns DJ. Geologic storage of hydrogen: scaling up to meet city transportation demands. Int J Hydrogen Energy Sep. 2014;39(28):15570–82. https://doi.org/10.1016/j.ijhydene.2014.07.121.
- [40] Papadias DD, Ahluwalia RK. Bulk storage of hydrogen. Int J Hydrogen Energy Oct. 2021;46(70):34527–41. https://doi.org/10.1016/j.ijhydene.2021.08.028.

- [41] Louis L. Four ways to store large quantities of hydrogen. Dec. 2021. https://doi. org/10.2118/208178-MS.
- [42] Olaf Kruck, Fritz Crotogino, Ruth Prelicz, and Tobias Rudolph, "Deliverable 3.1 -Overview of all known underground storage technologies," HYUNDER, pp25–37, 2013. Accessed: July. 31, 2022. [Online]. Available: http://hyunder.eu/publications/
- [43] Reuß M, Grube T, Robinius M, Preuster P, Wasserscheid P, Stolten D. Seasonal storage and alternative carriers: a flexible hydrogen supply chain model. Appl Energy Aug. 2017;200:290–302. https://doi.org/10.1016/j. apenergy.2017.05.050.
- [44] Amos WA. "Costs of storing and transporting hydrogen,". Jan. 1999. https://doi. org/10.2172/6574. NREL/TP-570-25106, ON: DE00006574, 6574.
- [45] Thomas G, Parks G. Potential roles of ammonia in a hydrogen economy. U.S. Department of Energy; 2006 [Online]. Available: https://www.energy.gov/sites/prod/files/2015/01/f19/fcto_nh3_h2_storage_white_paper_2006.pdf.
- [46] Hirscher M. Handbook of hydrogen storage: new materials for future energy storage | wiley. Wiley [Online], https://www.wiley.com/en-gb/Handbook+of+Hy drogen+Storage%3A+New+Materials+for+Future+Energy+Storage-p -9783527322732. [Accessed 1 August 2022].
- [47] Stewart M. 7 compressor fundamentals. In: Stewart M, editor. Surface production operations. Boston: Gulf Professional Publishing; 2019. p. 457–525. https://doi. org/10.1016/B978-0-12-809895-0.00007-7.
- [48] Alekseev A. Hydrogen liquefaction. In: Hydrogen science and engineering: materials, processes, systems and technology. John Wiley & Sons, Ltd; 2016. p. 733–62. https://doi.org/10.1002/9783527674268.ch30.
- [49] Berstad D, Skaugen G, Wilhelmsen Ø. Dissecting the exergy balance of a hydrogen liquefier: analysis of a scaled-up claude hydrogen liquefier with mixed refrigerant pre-cooling. Int J Hydrogen Energy Feb. 2021;46(11):8014–29. https://doi.org/ 10.1016/j.ijhydene.2020.09.188.
- [50] U.S. Department of Energy. Current status of hydrogen liquefaction costs. 2019 [Online]. Available: https://www.hydrogen.energy.gov/pdfs/19001_hydrogen_liquefaction_costs.pdf. [Accessed 30 July 2022].
- [51] Rouwenhorst KHR, Van der Ham AGJ, Lefferts L. Beyond Haber-Bosch: The renaissance of the Claude process. Int J Hydrogen Energy Jun. 2021;46(41): 21566–79. https://doi.org/10.1016/j.ijhydene.2021.04.014.
- [52] Semaskaite V, Bogdevicius M. Liquefied natural gas regasification technologies. 2022. p. 270–80. https://doi.org/10.1007/978-3-030-94774-3 27.
- [53] Wang L, et al. Greening ammonia toward the solar ammonia refinery. Joule Jun. 2018;2(6):1055-74. https://doi.org/10.1016/j.joule.2018.04.017.
- [54] Stolzenburg K, Mubbala R. Integrated design for demonstration of efficient liquefaction of hydrogen (IDEALHY). 2013 [Online]. Available: https://www. idealhy.eu/uploads/documents/IDEALHY_D3-16_Liquefaction_Report_web.pdf. [Accessed 30 July 2022].
- [55] Argonne National Laboratory and U.S. Department of Energy. Hydrogen delivery scenario analysis model [Online]. Available: https://hdsam.es.anl.gov/index.php? content=hdsam. [Accessed 30 July 2022].
- [56] Cardella UF. Large-scale hydrogen liquefaction. 2018. p. 192.
- [57] Lazard L. Lazard's levelized cost of hydrogen analysis. version 3, 2023.
- [58] Bertuccioli L, Chan A, Hart D, Lehner F, Madden B, Standen E. Development of water electrolysis in the European union [Online]. Available: https://www.fch.europa.eu/node/783. [Accessed 28 April 2022].
- [59] Azzaro-Pantel C. Hydrogen supply chain design, deployment, and operation. first ed. Academic Press; 2018 [Online]. Available: https://www.elsevier.com/books/h ydrogen-supply-chain/azzaro-pantel/978-0-12-811197-0. [Accessed 15 July 2022]
- [60] U.S. Department of Energy, "H2A Hydrogen Delivery Infrastructure Analysis Models and Conventional Pathway Options Analysis Results - Interim Report," pp. 2–49, 2014. Accessed: July. 30, 2022. [Online]. Available: https://www.energy.gov/eere/fuelcells/downloads/h2a-hydrogen-delivery-infrastructure-analysis-models-and-conventional.
- [61] Green DW, Perry RH. Perry's chemical engineers' handbook. eighth ed. McGraw-Hill Education; 2008 [Online]. Available: https://www.accessengineeringlibrary.com/content/book/9780071422949. [Accessed 30 July 2022].
- [62] Khan M.A., Mackinnon C., Layzell D. Technical brief: the techno-economics of hydrogen compression [Online]. The Transition Accelerator, pp. 13–15, Oct. 2021. https://transitionaccelerator.ca/techbrief-techno-economics-hydrogen-compre ssion/. [Accessed 27 July 2022].
- [63] International Energy Agency. "Macro drivers world energy model analysis," IEA [Online], https://www.iea.org/reports/world-energy-model/macro-drivers. [Accessed 9 June 2022].
- [64] Smith E, Morris J, Kheshgi H, Teletzke G, Herzog H, Paltsev S. The cost of CO2 transport and storage in global integrated assessment modeling. Int J Greenh Gas Control Jul. 2021;109:103367. https://doi.org/10.1016/j.ijggc.2021.103367.
- [65] Gas Infrastructure Europe and Guidehouse, "Picturing the value of underground gas storage to the European hydrogen system," p. 41, Jun. 2021. Accessed: July. 26, 2022. [Online]. Available: https://www.gie.eu/gie-presents-new-study-pictur ing-the-value-of-underground-gas-storage-to-the-european-hydrogen-system/.
- [66] Reddi K, Elgowainy A, Rustagi N, Gupta E. Techno-economic analysis of conventional and advanced high-pressure tube trailer configurations for compressed hydrogen gas transportation and refueling. Int J Hydrogen Energy Mar. 2018;43(9):4428–38. https://doi.org/10.1016/j.ijhydene.2018.01.049.